WP2 – Enhancing knowledge and data on gases and evaporators

D2.3 – Experimental study on evaporation from a chemical slick

Laura Cotte[1], Laurent Aprin[2], Clémence Prétat[1], Clémentine Kerleguer[1], William Giraud[1] and Stéphane Le Floch[1]

[1]Cedre, Research Department, 715 rue Alain Colas, F-29218 Brest CEDEX 2, France

[2]ARMINES-IMT Ales, Laboratory for the Science of Risks (LSR), 6 Avenue de Clavieres, 30100 Ales, France

Co-funded by the European Union

PAGE INTENTIONALLY LEFT BLANK

Co-funded by the European Union

ACKNOWLEDGEMENT

The work described in this report was supported by the Directorate-General for European Civil Protection and Humanitarian Aid Operations (DG-ECHO) of the European Union through the Grant Agreement number 101004912 - MANIFESTS – UCPM-2020-PP-AG, corresponding to the Call objective "Enhancing prevention and protection from the effects of maritime disasters" under priority 1: "Developing response capacity for marine pollution".

DISCLAIMER

PAGE INTENTIONALLY LEFT BLANK

Co-funded by the European Union

Project Acronym	**MANIFESTS**
Project Full Title	**MAN**aging risks and **I**mpacts **F**rom **E**vaporating and gaseous **S**ubstances To population **S**afety
Gant Agreement Nr.	**101004912**
Project Website	**https://www.manifests-project.eu/**

Deliverable Nr.	D2.3
Status (Final/Draft/Revised)	FINAL
Work Package	2
Task Number	2.3
Responsible Institute	ARMINES
Author/s	Laura Cotte, Laurent Aprin
Recommended Citation	Laura Cotte, Laurent Aprin, Clemence Pretat, Clementine Kerleguer, William Giraud and Stephane Le Floch (2023). Experimental study on evaporation from a chemical slick. MANIFESTS deliverable D2.3, 62pp.
Dissemination Level	Public

Document History			
Version	**Date**	**Modification Introduced**	
		Modification Reason	**Modified by**
1	15/12/2022	Draft sent for review to partners	Cedre
1.1	19/12/2022	Revision	UKHSA and RBINS
1.2	20/12/2022	Revision	ARMINES – IMT Alès
2	21/12/2022	Finalisation	Cedre
2	Early January 23	Internal proofreading	Cedre
FINAL	23/01/2023	Operational conclusions	Cedre

PAGE INTENTIONALLY LEFT BLANK

Co-funded by the European Union

Table of contents

PAGE INTENTIONALLY LEFT BLANK

Co-funded by the European Union

1. Executive summary

1.1. Behaviour of Hazardous and Noxious Substances (HNS)

Maritime transport of Hazardous and Noxious Substances (HNS) keep rising with a great variety of chemicals transported such as volatile and gaseous substances. The accidental release of such substances at sea can lead to the formation of toxic gas plumes that are still challenging for marine pollution authorities. So far, the risks for responders as well as the adequate response techniques to be used are poorly-known. Here the mechanisms driving the evaporation and dissolution of 6 chemicals from a slick on water surface were investigated through experimental tests at various scales. Results indicate that:

- On one hand evaporation induces a sharp decrease of temperature that tends to reduce vapour pressure and, hence, evaporation. On the other hand, the increase of wind velocity generally enhances evaporation kinetics as evidenced by higher vapour mass flow rates from water surface to the air;

- When released at the surface of seawater, the same chemicals displayed different behaviours and evaporation rates which were dependent on their vapour pressure and solubility in water;

- The most soluble chemicals presented the fastest dissolution kinetics and were not impacted significantly by increased salinity. On the contrary, the least soluble presented the slowest dissolution kinetics and higher solubility limits in freshwater than in salty water (20 and 35 ‰), in line with the 'salting' out effect and the SEBC. Four mathematical relationships that model the conjugate effect of temperature and salinity on solubility are now available for model parametrisation.

1.2. Operational aspects

- In the range of 5-30°C, the 6 chemicals studied will generally form a slick that will float at sea surface for a longer or shorter period of time, depending on their volatility.

- Due to their low viscosity and surface tension, the 6 chemicals studied will form a surface slick that will spread substantially, particularly in the open sea.

- Tests confirmed the theoretical behaviours described by the SEBC for five of the six chemicals studied, namely acrylonitrile (DE), ammonia aqueous (DE), cyclohexane (E), ETBE (E), petroleum benzine (FE). However, for vinyl acetate (ED), the observed experimental behaviour appeared more driven by the evaporation process than suggested by the SEBC.

- Based on the wind tunnel experiment, increasing wind velocities involves higher evaporation rates of chemicals, i.e. a faster evaporation of the slick.

- The experiment conducted using the chemistry test bench enabled to confirm that the evaporation kinetics is faster than the dissolution kinetics.

- In case of a release of a mixture of chemicals at sea the main priority is to check what are the substances involved and the risk of chemical reactions. Depending on the chemicals, azeotropic mixtures can form, involving either lower or greater boiling temperature than that of the pure constituents. Lower boiling temperatures means greater and quicker risks of evaporation of the slick with associated toxic gas plumes. Wearing of appropriate PPE is thus highly recommended in such cases.

2. Introduction

2.1. Context

Maritime transport represents more than 80% of the international trade volume (UNCTAD 2017). Apart from crude oil, tanker trades of refined petroleum products, chemicals and gas have increased by 4% over the 2019-2021 period, with a 5.6% growth in Liquefied Natural Gas (LNG) trade (UNCTAD 2022). The volume of hazardous and noxious substances (HNS) is thus constantly rising with an increased risk of accidental spillages potentially associated with marine pollutions, whether in ports or in the open sea. In the event of an incident and a spill in the environment, information on the fate of the chemical(s) involved is essential to better anticipate the risks incurred by responders and populations, the impacts on the environment as well as the appropriate response techniques (Mamaca et al. 2009).

Chemicals accidentally spilled into the marine or aquatic environment generally undergo physical-chemical modifications that will characterize their behaviour and fate. As observed by Mamaca et al. (2004) and Le Floch et al. (2011), these modifications are dependent on the intrinsic parameters of the product involved, the *in situ* environmental parameters (temperature, density and salinity of the water) and the meteo-ocean conditions (e.g. sea state, wind speed, marine currents). A few hours following the spill short-term effects may thus occur such as spreading, natural dispersion in the water column (dissolution, emulsification) and evaporation into the atmosphere. Longer term degradation (e.g. polymerisation, biodegradation) and sedimentation processes can then follow, depending on the persistence and the nature of the substance.
One of the main concern is that around 2,000 different types of HNS are regularly shipped in bulk or package forms (Purnell 2009) which thus make difficult to capture their behaviour if accidentally released in the environment.

Of the wide variety of HNS traded, volatile and gaseous substances are particularly problematic for marine pollution response authorities. The release of such substances at sea can indeed lead to the formation of toxic, flammable or explosive gas plumes – sometimes invisible to the naked eye – that can travel large distances and pose risks over a wide area in relatively short timescales. Yet, key information on the risks that responders or rescue teams could take when intervening, or those that could impact coastal communities and the environment when allowing a shipping casualty to dock at a place of refuge remain poorly-known. The MANIFESTS EU-project is part of this context.

2.2. Objectives of the study

The aim of this work was to enhance knowledge of the mechanisms involved in the evaporation of a chemical from a slick on the water surface through a series of experimental tests at various scales. The experimental work was conducted in Cedre facilities on six HNS and organised in five stages:

1. Measurement of the physical properties at i) standard conditions (atmospheric pressure, 20°C and in freshwater) to assess the reliability of data available in literature and ii) various temperatures;

2. Determination of the evaporation kinetics in the laboratory at standard conditions (atmospheric pressure, 20°C and no wind applied) for i) pure chemicals, ii) chemicals spilt at seawater surface and iii) binary mixtures;

3. Characterisation of the impact of wind speed on the evaporation kinetics using the wind tunnel developed by Cedre in the framework of the MANIFESTS project. Calculation of the vapour mass flow rate from water surface to the air;

4. Determination of the dissolution kinetics and the solubility limits of 4 HNS and establishment of a mathematical relationship modelling solubility as a function of temperature and salinity;

5. Evaluation of the competition between evaporation and dissolution using Cedre's chemistry test bench.

All results are presented in this report and will be incorporated into the HNS database developed by Cedre and its partners (https://manifests-project.eu/hns-database/).

3. Results and discussion

All material and methods used in this study are presented in Appendix 1.

3.1. Physical properties

3.1.1. Specific gravity

Specific gravities were measured using an Anton Paar density meter (DMA 4500 M) and are provided in Table 1. The experimental data measured at 20°C are in agreement with literature data with gaps smaller than 1.5 %. All specific gravities measured were lower than 1, indicating that the 6 chemicals studied will remain at sea surface after release. As expected an increase in temperature led to a decrease of specific gravity: the variation observed was in the range of 2 – 3 % between 5 and 30°C.

Table 1. Specific gravities at 5, 10, 15, 20 and 30°C.

HNS	Specific gravity					
Temperature (°C)	**5**	**10**	**15**	**20**	**30**	**Literature (20°C)***
Acrylonitrile	0.824	0.819	0.813	0.806	0.799	0.810
Ammonia	0.897	0.894	0.893	0.889	0.888	0.900
Cyclohexane	0.793	0.788	0.784	0.780	0.772	0.778
Petroleum benzine (naphta)	0.786	0.783	0.779	0.776	0.770	0.770
Tert-Butyl Ethyl Ether (ETBE)	0.758	0.753	-	0.744	0.735	0.750
Vinyl acetate	0.951	0.945	0.940	0.933	0.923	0.930

*From HNS MS data base[1]

In the range of 5-30°C, the 6 chemicals studied will generally form a slick that will float at sea surface for a longer or shorter period of time, depending on their volatility.

3.1.2. Viscosity

Kinematic viscosities were measured using an Anton Paar rotational rheometer (RheolabQC) and are summarised in Table 2. As expected an increase in temperature resulted in a decrease of viscosity (Andrade 1930): the variation observed was in the range of 15 – 30 % between 5 and 30°C (Figure 1). Close viscosity values were found for acrylonitrile and vinyl acetate which is consistent with the data provided in literature (Table 2).

[1] https://manifests-project.eu/hns-database/

Table 2. Experimental viscosities measured at 5, 10, 15, 20 and 30°C.

HNS	Kinematic viscosity (cSt = 10^{-6} $m^2.s^{-1}$)					
Temperature (°C)	**5**	**10**	**15**	**20**	**30**	**Lit. 20°C**
Acrylonitrile	3.79	3.67	3.08	3.40	3.23	0.43
Ammonia	7.65	6.94	6.51	5.99	5.49	-
Cyclohexane	8.13	6.48	5.18	6.17	5.74	1.27
ETBE	< LoD	< LoD	-	< LoD	< LoD	0.53
Vinyl acetate	3.61	3.54	3.69	3.38	3.01	0.46
Petroleum benzine	6.03	5.97	5.72	5.52	5.15	-

However, experimental data are 4 to 9 times greater than values found in the literature. This gap was due to the experimental device: the viscosities to be measured were too low for the concentric cylinder system used. The purchase of a specific measuring module is currently being considered.

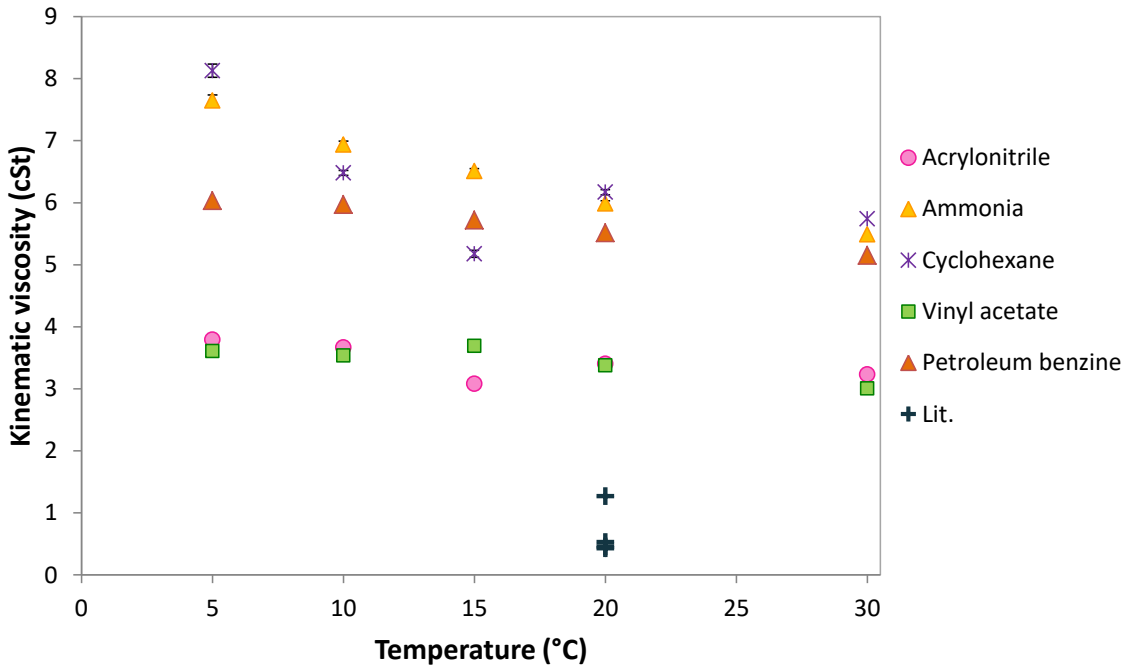

Figure 1. Evolution of the kinematic viscosity with temperature.

3.1.3. Surface tension

Surface tension was measured using the du Noüy ring method (Du Noüy 1919). The data collected are presented in Table 3. The experimental data measured at 20°C are in agreement with literature data with gaps smaller than 10 % (Figure 2). As expected an increase in temperature resulted in a decrease of surface tension (Palmer 1976). The decrease observed was in the range of 2 – 12 % between 5 and 30°C.

Table 3. Surface tension measured at 5, 10, 15, 20 and 30°C.The exact temperatures measured over each experiment are provided as it was often difficult to get the desired temperature.

HNS	Temperature	Surface tension γ	Stddv
	°C	$mN.m^{-1}$	$mN.m^{-1}$
Acrylonitrile	5.40	28.90	0
	9.20	27.91	0.01
	11.1	27.65	0.01
	15.3	27.75	0
	20.9	26.73	0
	30.3	25.44	0.01
Ammonia	5.00	60.58	0.01
	10.6	59.86	0.01
	15.8	59.75	0.01
	19.8	59.49	0.02
	24.8	59.29	0.03
Cyclohexane	11.9	24.94	0.01
	14.8	24.90	0.01
	17.1	24.62	0.01
	22.0	24.20	0.01
	29.7	23.60	0
Petroleum benzine (naphta)	6.0	25.58	0.02
	9.35	24.95	0.01
	12.8	24.73	0.01
	16.0	24.57	0.01
	20.6	24.16	0.01
	29.9	23.13	0
Tert-Butyl Ethyl Ether (ETBE)	5.70	19.45	0.01
	9.60	19.23	0.01
	12.3	19.12	0.01
	21.8	18.19	0.01
	28.6	17.52	0.01
	30.0	17.50	0.01
Vinyl acetate	5.40	25.06	0.01
	10.6	24.70	0.01
	14.7	23.83	0.01
	15.7	23.45	0.01
	21.0	23.80	0.01
	30.1	22.88	0

Due to their low viscosity and surface tension, the 6 chemicals studied will form a surface slick that will spread substantially, particularly in the open sea.

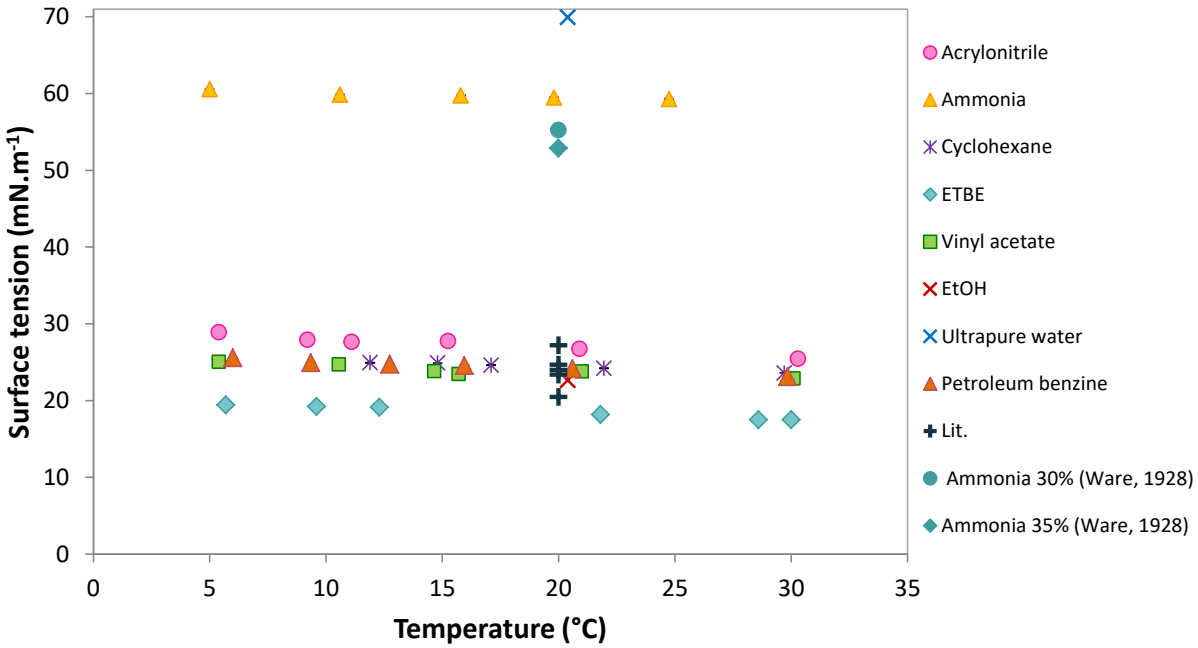

Figure 2. Evolution of surface tension (du Noüy ring method) with temperature. Literature data for ammonia are available in Ware (1928). Other literature data are available in the HNS-MS database.

3.2. Evaporation kinetics

The evaporation kinetics of the HNS listed in Appendix 1 (Table A) was investigated at two scales: in the lab at standard conditions and at pilot-scale using the wind tunnel. Tests in the lab included three stages: i) the evaporation of each chemical alone (pure), ii) the evaporation of each chemical at sea surface and iii) the evaporation of binary mixtures, without seawater. Pilot-scale experiments were then carried out using the wind tunnel. Results are presented in the following sections.

3.2.1. Evaporation of chemicals pure

In the given experimental conditions, all chemicals but ammonia showed a linear mass loss over time ($r^2 > 0.99$; Figure 3). In such cases the evaporation kinetics was equivalent to the opposite of the slope of the regression line. Results are summarised in Table 4.

Acrylonitrile, cyclohexane, ETBE and vinyl acetate had fully evaporated between 1 h 30 and 3 h after the beginning of the experiment. However, ammonia and petroleum benzine took more than 30 h to evaporate. Overall the chemicals studied displayed significantly higher evaporation kinetics than seawater (Figure 3). ETBE was the fastest to evaporate (1 h 30) with a mass flow of 4.9 $g.h^{-1}$. Vinyl acetate and cyclohexane both evaporated 2 h 30 after being spilt with a mass flow of 3.9 $g.h^{-1}$ and 3.2 $g.h^{-1}$, respectively. Acrylonitrile had fully evaporated in 3 h with a mass flow of 2.8 $g.h^{-1}$ while petroleum benzine mass flow was as low as 0.2 $g.h^{-1}$.

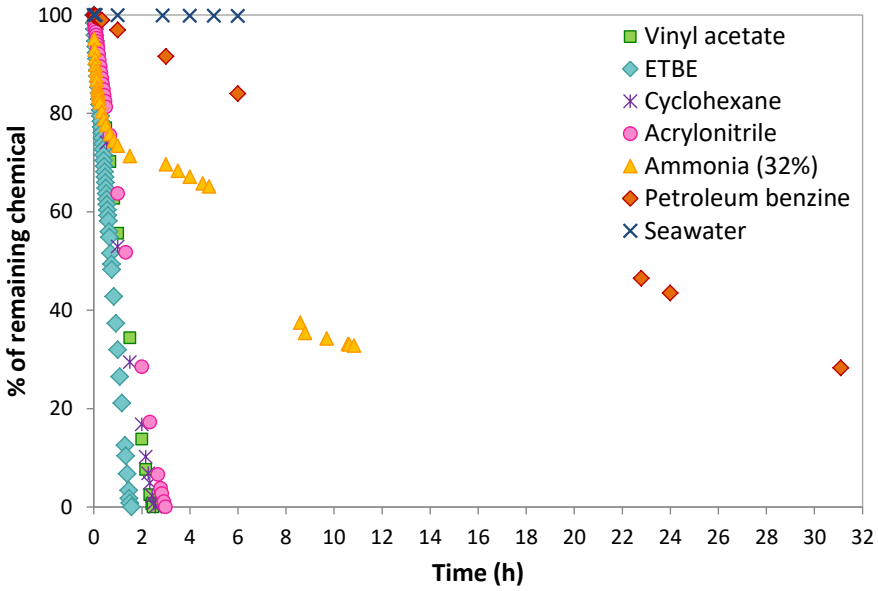

Figure 3. Monitoring of HNS mass loss with time. When the mass loss is linear, the evaporation kinetics is equivalent to the opposite of the slope of the regression line (except for ammonia).

The evaporation kinetics of these products was generally in agreement with the behaviour predicted by the SEBC classification. The case of ammonia was more complex as it was a mixture of ammonia and water. The first minutes seem to match with the evaporation of ammonia. Then the plateau reached at around 8 h after the spill highlights that almost only water remained in the crystallizer (Figure 3).

Table 4. Mass flow calculated. The grey frame is for the experiment conducted in seawater.

HNS	Mass flow HNS alone ($g.h^{-1}$)	Mass flow HNS at the surface of seawater ($g.h^{-1}$)	After 47 min ($g.h^{-1}$)	After 1 h ($g.h^{-1}$)	After 4 h ($g.h^{-1}$)	After 5 h ($g.h^{-1}$)
Artificial seawater	0,2	-	-	-	-	-
Acrylonitrile	2,8	1,5	-		0,4	-
Ammonia	7,5*	1,1	0,4	-	-	0,1
Cyclohexane	3,2	2,6	-	-	-	-
ETBE	4,9	9,6	-	-	-	-
Petroleum benzine	0,2	0,2	-	-	-	-
Vinyl acetate	3,9	9,9	-	0,3	-	-

*estimated

3.2.2. Evaporation of chemicals at sea surface

In this second stage, the mass evaporated was assessed by subtracting the initial weight of water to the mass weighed. The evaporation rate was then calculated as in 3.2.1 and compared to the results collected for the evaporation of chemicals alone.

For cyclohexane, ETBE and petroleum benzine the linearity was preserved ($r^2 > 0.99$) and a constant mass flow rate was observed over the experiment (Figure 4). This feature could be explained by the low hydrosolubility of cyclohexane and petroleum benzine (0.055 $g.L^{-1}$ and 0.04 $g.L^{-1}$, respectively): most of the slick could remain onto sea surface and evaporate without any significant dissolution process interfering during the experiment. Vapour pressure also favours greatly the evaporation process over dissolution. This is particularly the case for cyclohexane and ETBE (Appendix 1; Table A). Note that vapour pressure largely prevails over hydrosolubility in the behaviour observed, particularly for ETBE that did not seem to undergo significant dissolution process despite its high solubility in water (12 $g.L^{-1}$).

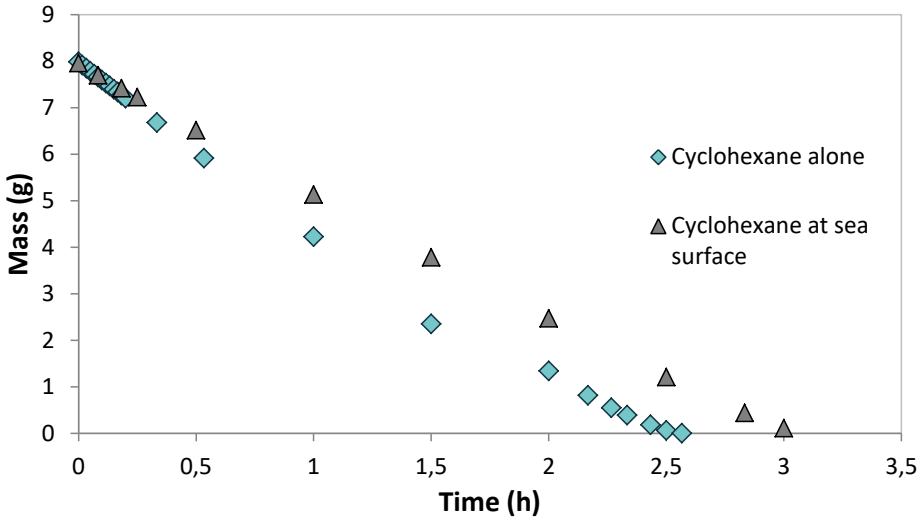

Figure 4. Comparison of the evaporation kinetics of cyclohexane alone and at sea surface.

In terms of mass flow, no difference was observed for petroleum benzine at sea surface. However, cyclohexane presented a 20 %-lower evaporation rate at sea surface than alone (Figure 4 and Table 4). Here slight dissolution of cyclohexane might explain the behaviour observed but not to the point of drastically changing the evaporation rate. Finally ETBE displayed a 50 %-higher evaporation rate when spilt at sea surface (Figure 5 and Table 4). When ETBE was spilt, water surface seemed to boil. Coupled with the high vapour pressure (20 kPa), such surface agitation might have helped to speed up the evaporation process.

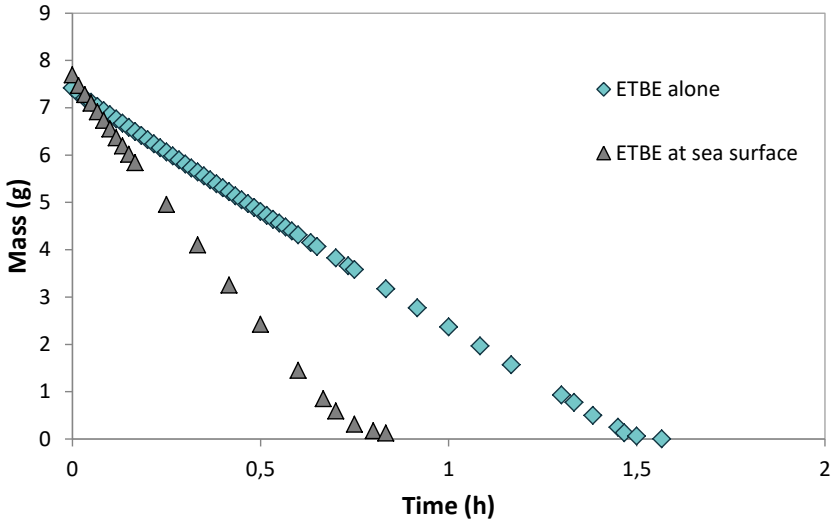

Figure 5. Comparison of the evaporation kinetics of ETBE alone and at sea surface.

A two-phase evaporation process was observed for acrylonitrile and vinyl acetate: both exhibited non-linear mass loss over time with generally longer mass flow rates (Table 4 and Figure 6). This might be linked to their greater affinity with water (20 $g.L^{-1}$ and 79 $g.L^{-1}$, respectively).

For acrylonitrile, the evaporation rate at sea surface was 1.9 times lower than for the chemical alone (1.5 $g.h^{-1}$ against 2.8 $g.h^{-1}$, Table 4). After 4 h the evaporation process was lower and the mass transfer dropped down to 0.4 $g.h^{-1}$. This suggests that, initially, most of the product dissolved in seawater and then gradually rose up to the surface before evaporating, in line with the behaviour predicted by the SEBC (DE). Regarding vinyl acetate, the evaporation rate at sea surface was 2.5 times higher than alone (9.9 $g.h^{-1}$ against 3.9 $g.h^{-1}$, Table 4). After 1 h the evaporation process slowed down sharply and the mass transfer dropped down to 0.3 $g.h^{-1}$. This suggests that most of the substance evaporated rapidly while the remaining part that was dissolved in seawater gradually rose up to the surface before evaporating, in line with the theoretical behaviour predicted by the SEBC (ED).

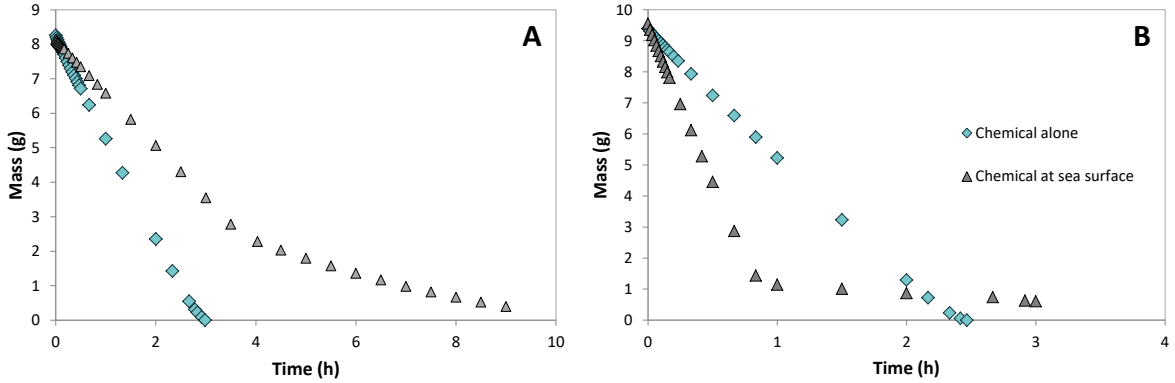

Figure 6. Comparison of the evaporation kinetics of A) acrylonitrile (DE) and B) vinyl acetate (ED) alone and at sea surface.

3.2.3. Evaporation of mixtures

Incidents involving leakages from one cargo to another or multiple leakages could bring risk of mixing incompatible chemicals. As pointed out by the MANIFESTS Advisory Board, the resulting hazards should not be neglected even though they are still poorly-known. Hence, pre-tests were performed on two binary mixtures to study the associated evaporation process (Table 5).

Table 5. Mixtures studied in the lab.

	Volume (mL)	Chemicals	
Mixture 1	20	Cyclohexane	Vinyl acetate
Mixture 2	20	Cyclohexane	Acrylonitrile

The evaporation rate of the first mixture was found to be very similar to cyclohexane and vinyl acetate alone (Figure 7). This suggests that, in these experimental conditions, each compound evaporates independently: no particular hazard is expected for this mixture (e.g. chemical reaction), apart from the effects of a combined exposure to these 2 chemicals.

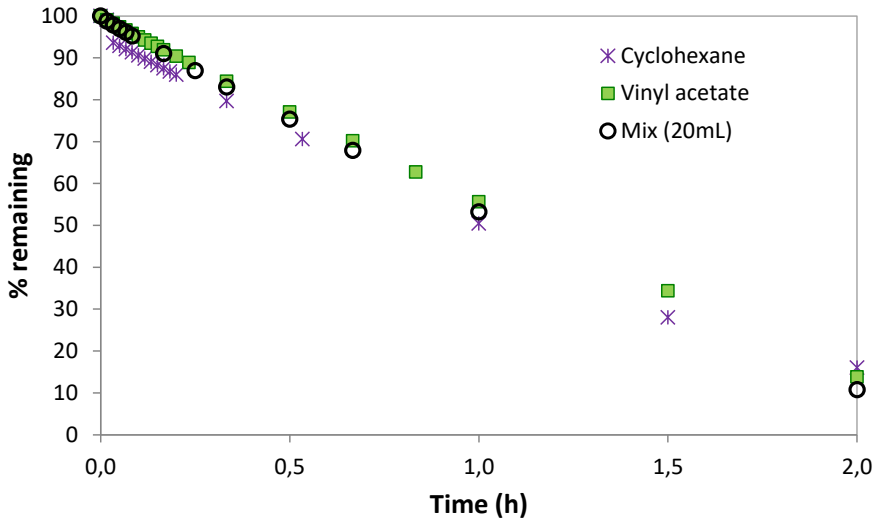

Figure 7. Evaporation of cyclohexane mixed with vinyl acetate (V_{tot} = 20 mL). Comparison with each chemical alone.

However, for the second mixture, the evaporation rate was closer to the one assessed for cyclohexane than for acrylonitrile (Figure 8). This might be due to the formation of an azeotropic mixture, i.e. a mixture that has the property of having a unique and defined boiling temperature for a given composition[2]. Such mixtures have certain physical properties that are those of pure bodies, and in particular the property of having the same composition in the gaseous and liquid phase. The azeotropic mixture is said to be 'positive' if its boiling temperature is lower than that of the pure

[2] https://www.universalis.fr/encyclopedie/melange-azeotrope/

constituents (negative in the opposite case). Hence, a positive azeotropic behaviour was suggested to explain the behaviour observed.

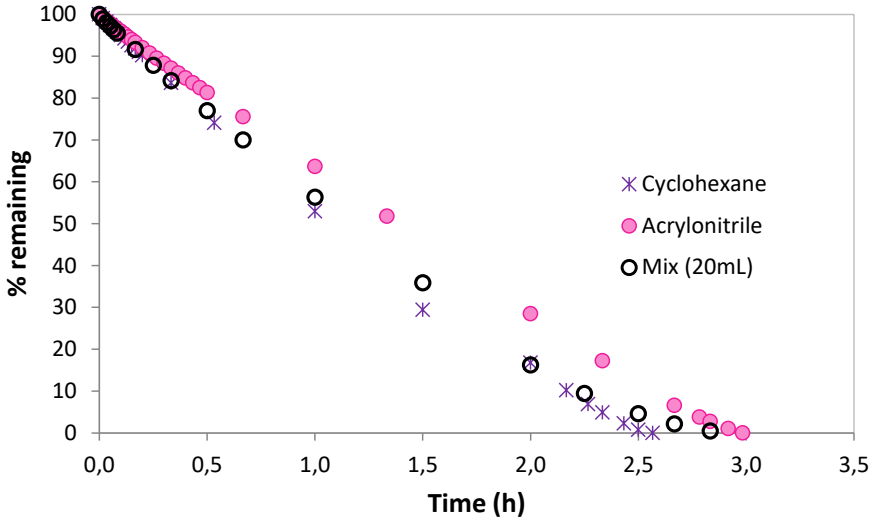

Figure 8. Evaporation of cyclohexane mixed with acrylonitrile (V_{tot} = 20 mL). Comparison with each chemical alone.

In the field, a positive azeotropic behaviour could lead to a greater risk of gas plume and, more importantly, faster than initially estimated by predictions models. Consequently the notion of azeotrope must be popularized to marine pollution authorities. Evaporation models can predict azeotropic mixtures but cannot specify whether it will be a positive or negative azeotropic behaviour. One possibility would be to display a warning message on available decision-support systems to first responders when there is a chance to form an azeotropic mixture.

- A positive azeotropic behaviour could lead to a greater risk of gas plume. The gas cloud may form faster than initially estimated by predictions models.
- Note that in case of mixture of chemicals at sea, a medical expert should be consulted to assess the possible effects of combined exposure to multiple chemicals. Expertise from industrial hazardous waste specialists is also required (Alcaroa et al. 2021).

3.2.4. Limitations of the experiment

The purpose of these lab tests was to calibrate the evaporation module developed in the framework of MANIFESTS (WP4 and WP5) in order to provide more precise information regarding the formation of toxic gas clouds (Go / No-Go decision). Though the first set of data collected in the lab was of interest for modellers, one critical parameter – the wind speed – has not been monitored during the experiments. Indeed, the mass flow rate J ($kg.m^{-2}.s^{-1}$) is given by the Mackay and Matsugu 1973 model which can be expressed as follows:

$$J = K_G.\frac{P_V.M}{R.T} \text{ with } K_G = 0.0048U_{wind}^{7/9}.X^{-1/9}.Sc^{-2/3} \text{ (Eq.1)}$$

Where

K_G: Mass transfer coefficient [$m.s^{-1}$]
P_V: Vapour pressure [Pa]
M: Molecular weight of the compound [$kg.mol^{-1}$]
R: Gas constant [$J.mol^{-1}.K^{-1}$]
T: Temperature [K]
U_{wind}: Wind speed [$m.s^{-1}$]
X: Pool diameter [m]
Sc: Schmidt number

Hence, when wind speed is null, the mass transfer coefficient K_G is also null and the model does not predict any evaporation process. To overcome this issue a wind tunnel was developed by Cedre with a great support of ARMINES-IMT Mines Alès. The experimental tool enabled to assess the impact of wind speed on the evaporation kinetics of HNS (see the experimental set up in Appendix 1; A1.1.2.2. Wind tunnel).

3.2.5. Wind tunnel

Experiment at constant wind velocity

The first test consisted in monitoring the mass variation over time of acrylonitrile, cyclohexane, petroleum benzine and vinyl acetate under a constant wind of 8 $m.s^{-1}$. Results are presented in Figure 9.

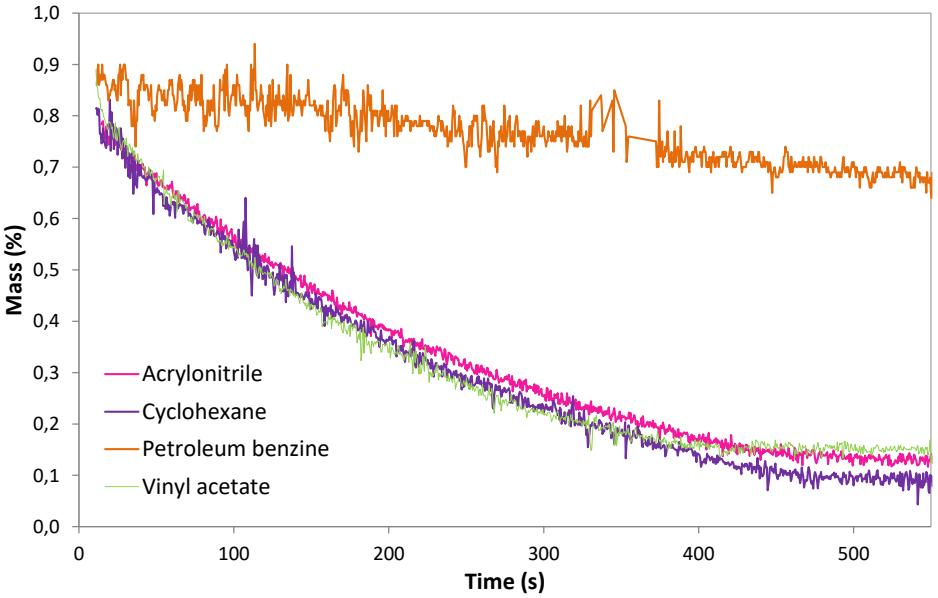

Figure 9. Evaporation of acrylonitrile, cyclohexane, petroleum benzine and vinyl acetate at constant wind velocity (8 $m.s^{-1}$). Timescale was shortened to allow comparison between all chemicals. The experiment performed with petroleum benzine last around 2 h.

Mass variation is similar for Acrylonitrile, cyclohexane and vinyl acetate with a polynomial law decrease whereas Petroleum benzine seems to decrease according to a linear law. After filling the petri-dish a sharp decrease of liquid temperature in the range of 10-15°C was observed for acrylonitrile, cyclohexane and vinyl acetate (Figure 10).

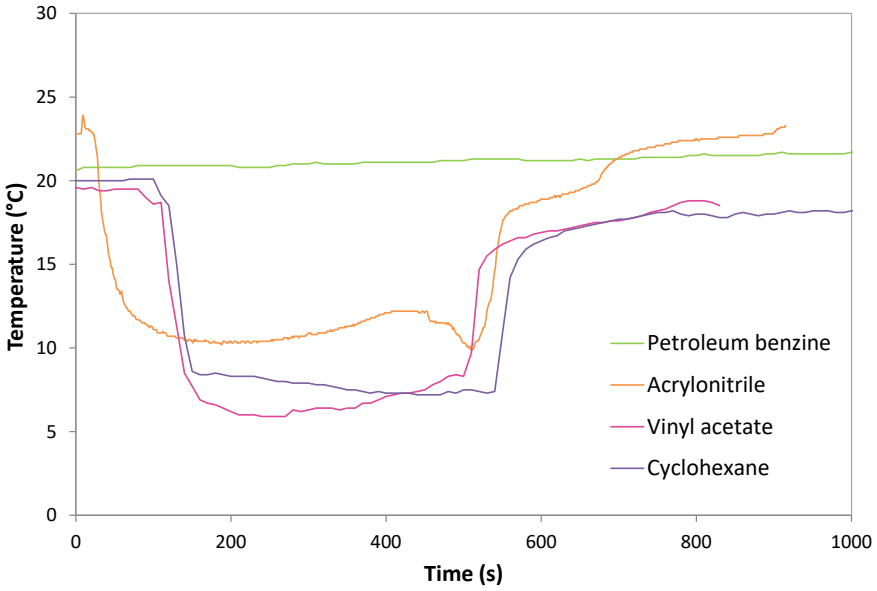

Figure 10. Liquid temperature over the evaporation process at constant wind velocities (8 $m.s^{-1}$).

When focusing on a narrow range of temperature, a drop of around 2°C was also noticed for petroleum benzine (Figure 11). In this case, a higher measurement frequency could be useful to enhance temperature data resolution (e.g. 2 Hz).

Evaporation is an endothermic process that absorbs energy, or heat, from the environment, thus lowering the energy level of the medium (Gonczi 2005). Here the heat loss was not compensated by sufficient heat exchange from the environment (air, solar intake, etc.). This transiently led to a drop in liquid temperature that tended to reduce vapour pressure and, hence, evaporation. This feature was already observed in previous works (e.g. Braconnier et al. 2008; Heymes et al. 2013). After 125 s for acrylonitrile, 160 s for cyclohexane 150 s for vinyl acetate and 2320 s (40 min) for petroleum benzine, the liquid temperature remained stable and the evaporation rate became constant (Figure 10 and Figure 11).

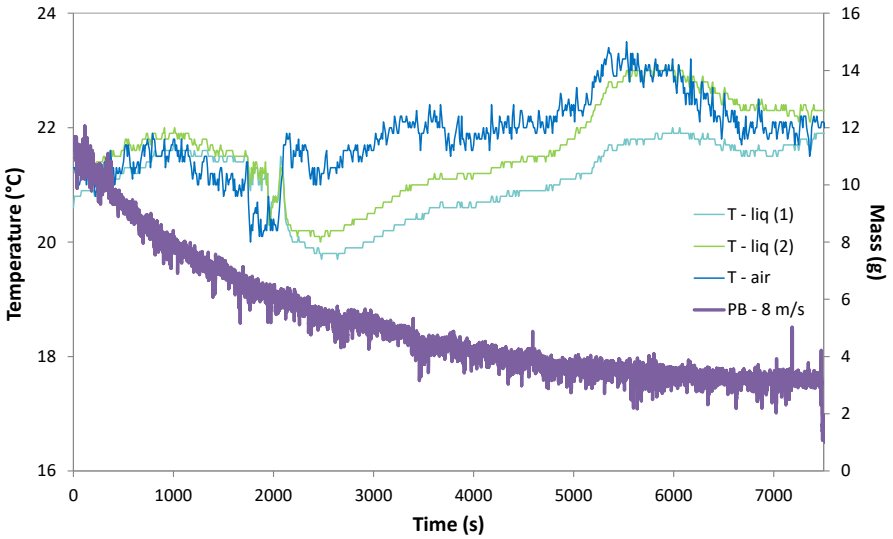

Figure 11. Evaporation of petroleum benzine at 8 $m.s^{-1}$ with associated air and liquid temperatures.

The mass flow rate J was calculated according to Eq.1. Vapour pressures were first derived from the Clausius-Clapeyron relationship. The vapour diffusion coefficients were calculated using a qualitative relation between the dimension of the petri-dish and the typical duration of the evaporation process, i.e. the time over which the liquid temperature remains constant. The dimensionless Schmidt number was then deduced from the kinematic viscosity of air ($m^2.s^{-1}$) divided by the vapour diffusion coefficient. This enabled to calculate the mass transfer constant K_G. Results are reported in Table 6.

Table 6. Physical properties and mass transfer constants at a wind velocity of 8 $m.s^{-1}$.

Parameter	Acrylonitrile	Cyclohexane	Petroleum benzine	Vinyl acetate
Vapour pressure (kPa)	10,89	10,10	0,70	12,62
Vapour diffusion coefficient ($m^2.s^{-1}$)	$3,17 \times 10^{-5}$	$2,46 \times 10^{-5}$	$1,87 \times 10^{-6}$	$2,66 \times 10^{-5}$
Schmidt number	0,50	0,65	8,55	0,60
Mass transfer coefficient K_G ($m.s^{-1}$)	$4,98 \times 10^{-2}$	$4,09 \times 10^{-2}$	$8,11 \times 10^{-3}$	$4,33 \times 10^{-2}$
Mass flow J ($g.m^2.s^{-1}$)	11,91	14,27	0,25	19,22

Table 7. Physical properties and mass transfer constants at different wind velocities for acrylonitrile.

Parameter	Wind velocity ($m.s^{-1}$)							
	0.5	1	2	3	4	7	8	10
Average air temperature (K)	294,14	294,50	294,88	294,01	295,31	296,33	296,50	297,57
Average liquid temperature (K)	290,27	289,29	290,90	290,41	291,12	289,36	290,74	293,18
Kinematic air viscosity ($m^2.s^{-1}$) *	$1,6 \times 10^{-5}$	$1,6 \times 10^{-5}$	$1,6 \times 10^{-5}$	$1,6 \times 10^{-5}$	$1,6 \times 10^{-5}$	$1,6 \times 10^{-5}$	$1,6 \times 10^{-5}$	$1,6 \times 10^{-5}$
Vapour pressure (kPa)	12,66	12,86	13,08	12,59	13,33	13,93	14,04	14,69
Vapour diffusion coefficient ($m^2.s^{-1}$)	$4,81 \times 10^{-6}$	$1,31 \times 10^{-5}$	$1,84 \times 10^{-5}$	$2,25 \times 10^{-5}$	$2,62 \times 10^{-5}$	$3,12 \times 10^{-5}$	$3,17 \times 10^{-5}$	$3,31 \times 10^{-5}$
Schmidt number	3,33	1,22	0,87	0,71	0,61	0,51	0,50	0,48
Mass transfer coefficient K_G ($m.s^{-1}$)	$1,64 \times 10^{-3}$	$5,64 \times 10^{-3}$	$1,19 \times 10^{-2}$	$1,86 \times 10^{-2}$	$2,55 \times 10^{-2}$	$4,43 \times 10^{-2}$	$4,98 \times 10^{-2}$	$6,09 \times 10^{-2}$
Mass flow J ($g.m^2.s^{-1}$)	0,45	1,57	3,38	5,10	7,34	13,29	15,05	19,19

Table 8. Physical properties and mass transfer constants at different wind velocities for cyclohexane. Note that wind velocities up to 15 m.s^{-1} were tested for this chemical.

Parameter	Wind velocity (m.s^{-1})										
	0.5	1	2	3	7	8	10	11	12	13	15
Average air temperature (K)	293,43	293,15	293,84	293,72	293,21	293,38	292,82	293,92	292,25	291,93	291,20
Average liquid temperature (K)	290,42	291,39	291,77	290,85	291,25	288,62	290,05	291,85	289,30	289,25	288,91
Kinematic air viscosity (m^2.s^{-1})*	1,6 x 10^{-5}	1,6 x 10^{-5}	1,6 x 10^{-5}	1,6 x 10^{-5}	1,6 x 10^{-5}	1,6 x 10^{-5}	1,6 x 10^{-5}	1,6 x 10^{-5}	1,6 x 10^{-5}	1,6 x 10^{-5}	1,6 x 10^{-5}
Vapour pressure (kPa)	10,13	9,99	10,32	10,26	10,02	10,10	9,85	10,36	9,59	9,45	9,13
Vapour diffusion coefficient (m^2.s^{-1})	6,36 x 10^{-6}	1,24 x 10^{-5}	1,68 x 10^{-5}	2,34 x 10^{-5}	2,85 x 10^{-5}	2,46 x 10^{-5}	2,40 x 10^{-5}	2,52 x 10^{-5}	2,46 x 10^{-5}	2,52 x 10^{-5}	2,59 x 10^{-5}
Schmidt number	2,51	1,29	0,95	0,68	0,56	0,65	0,67	0,63	0,65	0,63	0,62
Mass transfer coefficient K_G (m.s^{-1})	2,00 x 10^{-3}	5,22 x 10^{-3}	1,12 x 10^{-2}	1,88 x 10^{-2}	4,14 x 10^{-2}	4,09 x 10^{-2}	4,89 x 10^{-2}	5,47 x 10^{-2}	5,83 x 10^{-2}	6,23 x 10^{-2}	7,12 x 10^{-2}
Mass flow J (g.m^2.s^{-1})	0,70	1,80	3,97	6,65	14,32	14,27	16,64	19,52	19,37	20,40	22,61

*Kinematic air viscosity is from Heymes et al. (2013).

At constant wind conditions, the mass flow rates were the highest for vinyl acetate (19.22 $g.m^2.s^{-1}$), cyclohexane (14.27 $g.m^2.s^{-1}$) and acrylonitrile (11.91 $g.m^2.s^{-1}$) and the lowest for petroleum benzine (0.25 $g.m^2.s^{-1}$). This is fully in agreement with the evaporation rates estimated for lab tests (Table 4).

Experiment at increasing wind velocities

The second test enabled to study the evaporation process of acrylonitrile and cyclohexane at increasing wind velocities in the range of 0.5 to 11 $m.s^{-1}$. Physical properties and mass flow rate are reported in Tables 7 and 8. Mass losses of acrylonitrile and cyclohexane versus time for different wind velocities are presented in Figures 12 and 13, respectively. A typical representation of the mass loss recorded at one wind velocity and coupled to the corresponding air and liquid temperature is also shown as an example (Figure 14). Temperature profiles are reported in Figures 14, 15, 16 and 17.

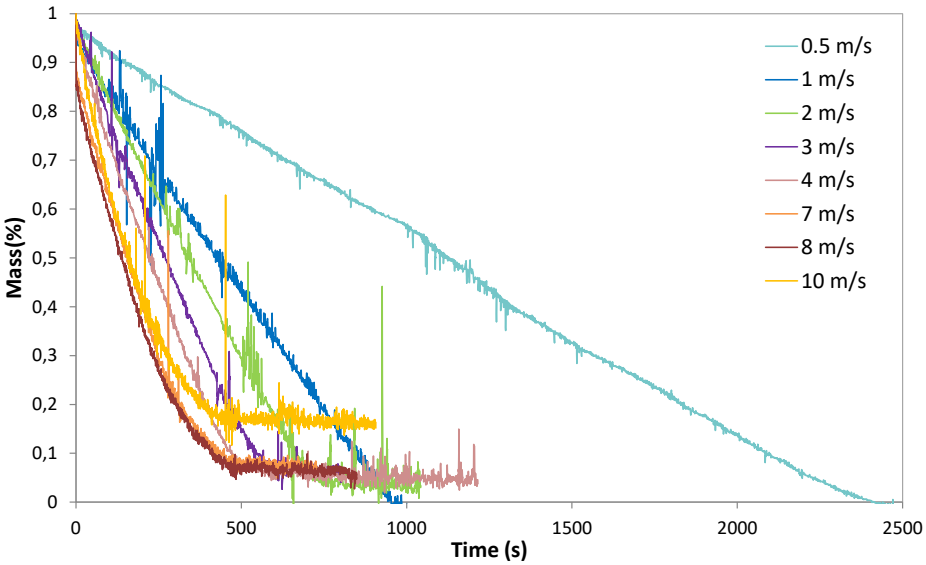

Figure 12. Evaporation rate of acrylonitrile at different wind velocities.

As observed for lab tests, acrylonitrile and cyclohexane generally presented a linear mass loss over time. Mass also decreased faster with increasing wind velocities as evidenced by steeper slopes (Figures 12 and 13). This suggests that an increase in wind velocity generally involves higher evaporation rates.

Above the apparent thresholds of 7 $m.s^{-1}$ for acrylonitrile and 5 $m.s^{-1}$ for cyclohexane the evaporation rate seemed to stagnate as the slopes did not seem anymore to increase proportionally with the wind velocity. A rapid saturation of the air with vapours of the chemical investigated might partly explain this phenomenon. But, above all, the evaporation process could have been hindered by the sharp decrease in temperature that was often greater than 10°C (Figures 15, 16 and 17). In the case of cyclohexane, the temperature drop is such that it reaches a temperature close to 6-7°C, i.e. close

the cyclohexane's melting point. From 2 m.s^{-1} and up to 11 m.s^{-1} cyclohexane crystals were indeed observed in the petri-dish as it started freezing (Figure 16).

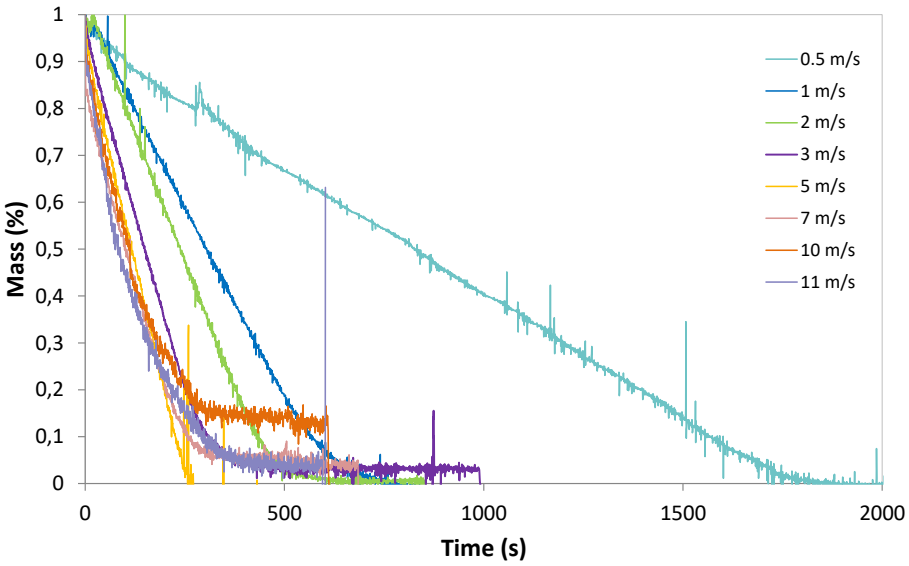

Figure 13. Evaporation rate of cyclohexane at different wind velocities.

Surprisingly, the mass flow rates calculated do not reflect any clear 'stagnation' of the evaporation kinetics at high wind conditions (Figures 18 and 19). However, as observed by Bogeshwaran et al. (2015) for the diffusion of hexane in the air, increasing wind velocities clearly affects diffusion: the vapour diffusion coefficient increases up to a threshold value reached at stronger wind conditions (Figures 18 and 19). More investigation is thus still needed to secure the experimental mass flow rate obtained in this work.

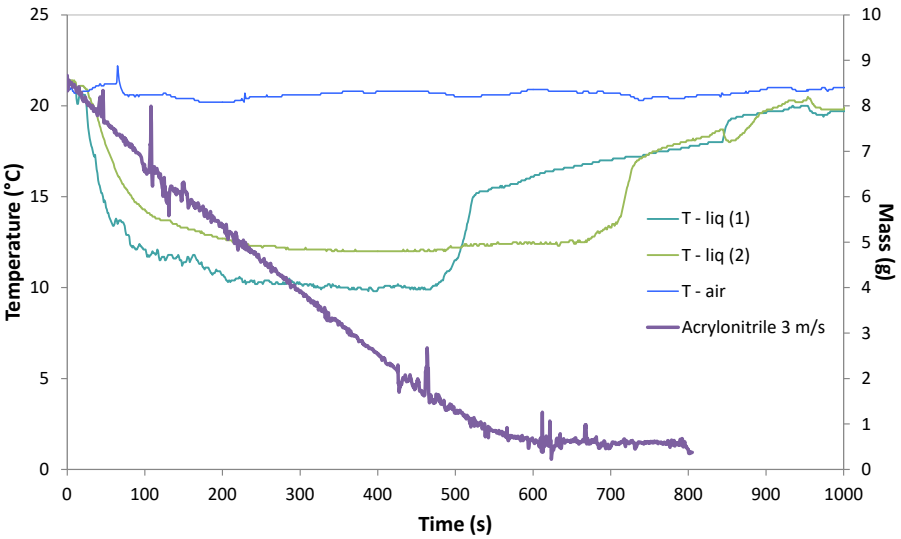

Figure 14. Evaporation of acrylonitrile at 3 m.s^{-1} with associated air and liquid temperatures.

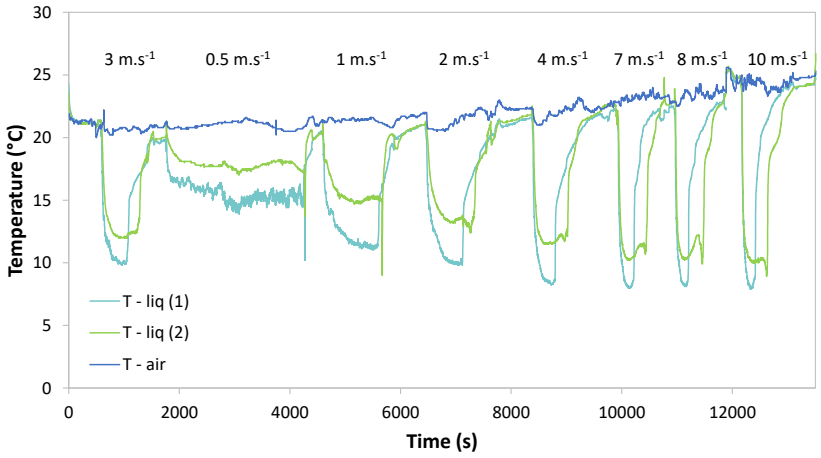

Figure 15. Air and liquid temperatures during the evaporation of acrylonitrile at various wind velocities.

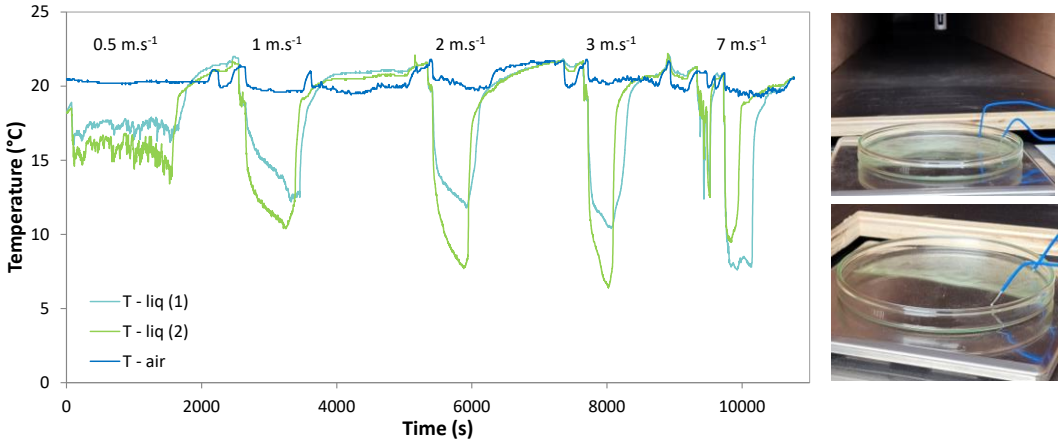

Figure 16. Air and liquid temperatures during the evaporation of cyclohexane at various wind velocities. On the right picture, cyclohexane crystals can be observed in the petri-dish as it starts freezing.

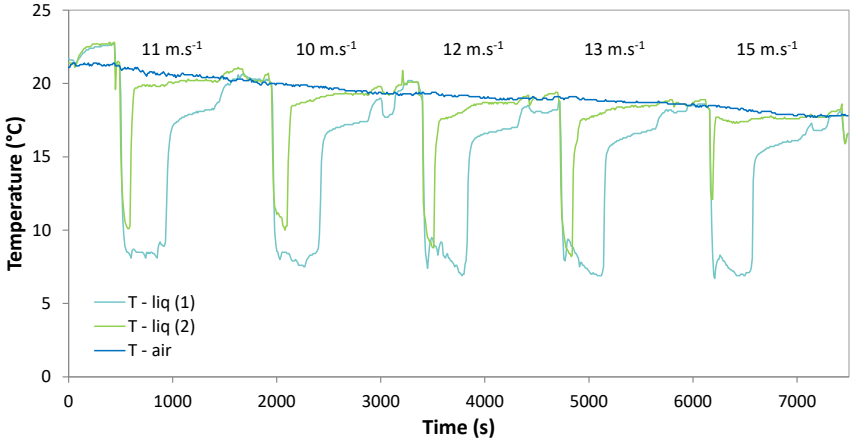

Figure 17. Air and liquid temperatures during the evaporation of cyclohexane at higher wind velocities (10-15 $m.s^{-1}$).

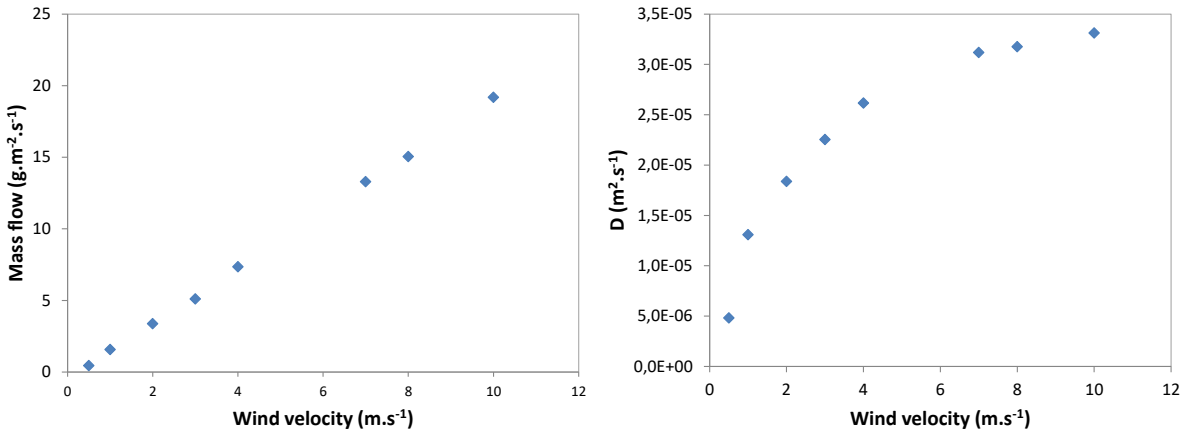

Figure 18. Mass flow and vapour diffusion coefficient with increasing wind velocities (acrylonitrile).

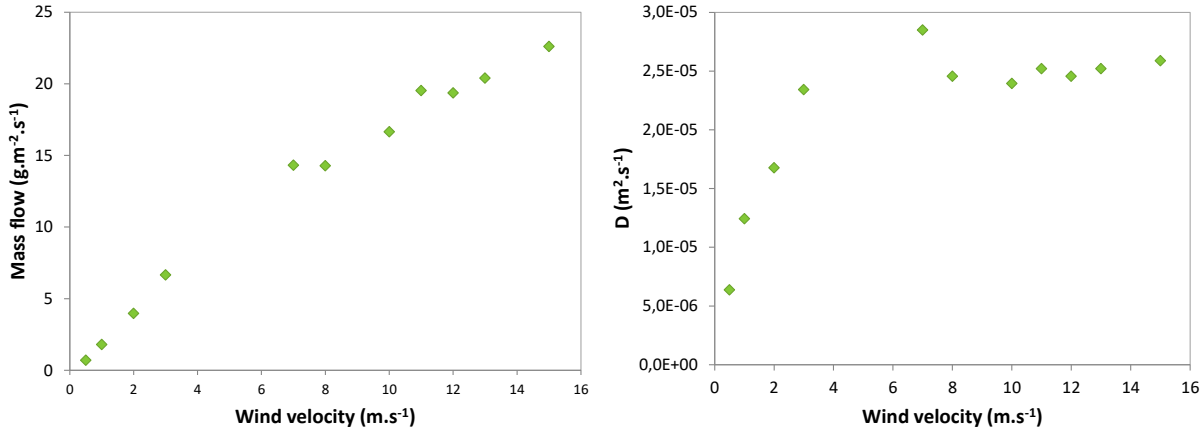

Figure 19. Mass flow and vapour diffusion coefficient with increasing wind velocities (cyclohexane).

Tests were finally performed on seawater alone in preparation for future work to determine the evaporation kinetics of the same chemicals, but spilt at seawater surface (~ 500 mL). Data collected are still under processing. Results obtained will allow estimating the proportion of seawater that evaporates during such tests and making appropriate corrections to recover the evaporation kinetics of each HNS.

- Evaporation transiently leads to a drop in liquid temperature. This temperature variation should not be so important in real environmental conditions.
- An increase in wind velocity generally involves higher evaporation rates.

3.3. Dissolution

The hydrosolubility of acrylonitrile, cyclohexane, petroleum benzine and vinyl acetate was characterised for different conditions of temperature and salinity of the aqueous phase. The data collected enabled to establish a mathematical relationship that models the conjugate effect of temperature and salinity on the hydrosolubility of each chemical. Similar work was performed earlier for dimethyldisulfide (DMDS), methyl methacrylate (MMA), methyl ethyl ketone (MEK) and 1-butanol (Benbouzid et al. 2012). Such experimental data play a significant part in providing a clearer picture on the conduct to be adopted in case of spills at sea.

3.3.1. Analytical performance

Detection limits are presented in Table 9. The lowest concentrations measured in the first aliquots were generally well above the LOD except for cyclohexane and petroleum benzine because of their low solubility in water. Blanks were negligible compared to samples. All calibration lines were characterised by a high correlation coefficient ($r^2 > 0.99$).

Table 9. Detection limits of the analytical method.

	Acrylonitrile	Cyclohexane	Petroleum benzine	Vinyl acetate
LOD ($g.L^{-1}$)	0.006	0.001	0.006	0.058
LOQ ($g.L^{-1}$)	0.016	0.003	0.021	0.126

3.3.1. Dissolution kinetics

The dissolution kinetics was defined as the time required to reaching the concentration plateau (Appendix 1; A1.1.3.3. Expected results).

Similar trends were observed for the four chemicals investigated: a sharp increase of the concentrations during the first hours of the experiment until stabilisation up to the concentration plateau. The fastest kinetics was observed for acrylonitrile and vinyl acetate with a concentration plateau reached after 8 hours whatever temperature or salinity conditions (e.g. Figure 20 and Figure 21). For cyclohexane and petroleum benzine 24 and 48 hours were needed whatever temperature or salinity of the aqueous phase (Figure 22 and Figure 23). This is consistent with the SEBC.

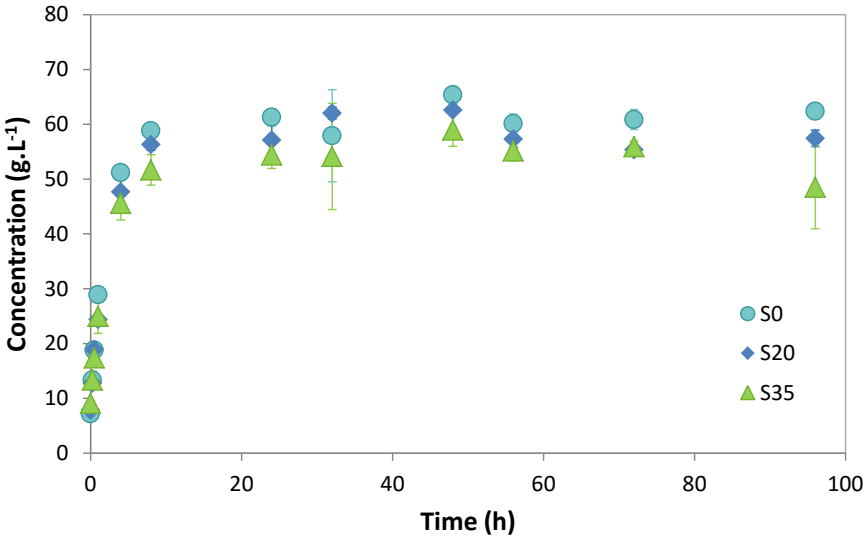

Figure 20. Concentration measured at 15°C for acrylonitrile in freshwater and saline solutions versus time.

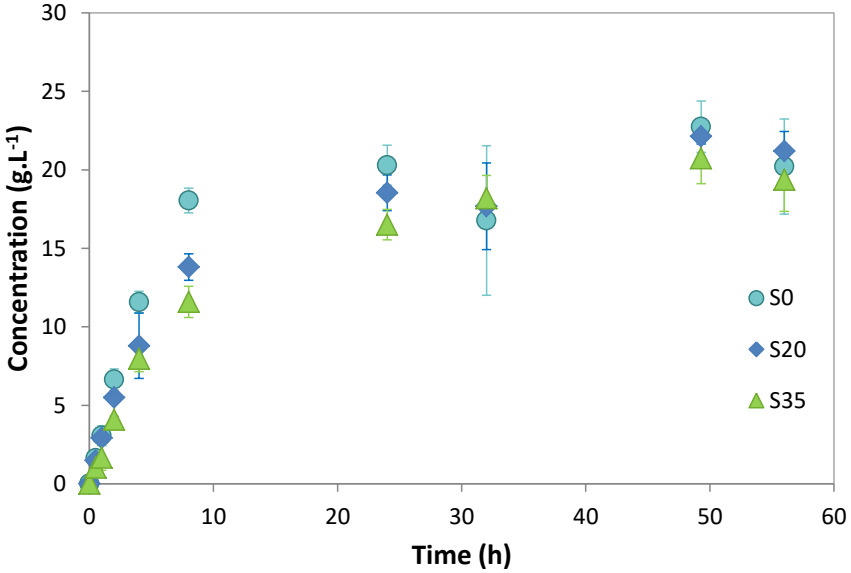

Figure 21. Concentration measured at 25°C for vinyl acetate in freshwater and saline solutions versus time.

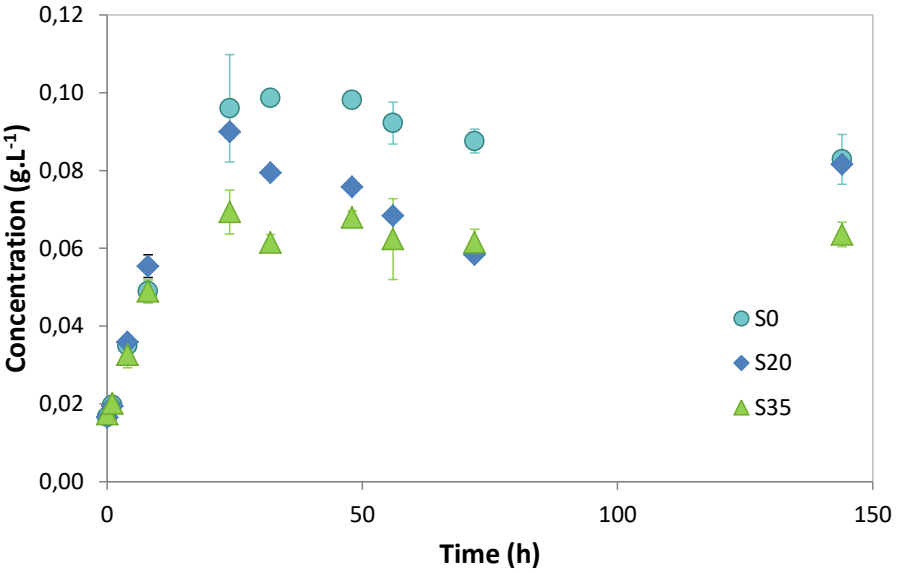

Figure 22. Concentration measured at 15°C for cyclohexane in freshwater and saline solutions versus time.

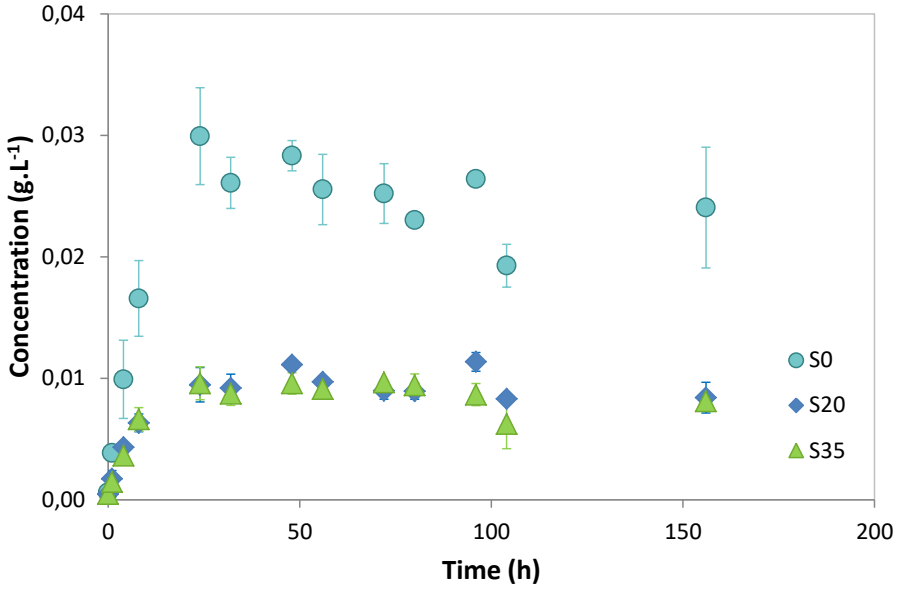

Figure 23. Concentration measured at 20°C for petroleum benzine in freshwater and saline solutions versus time.

3.3.2. Solubility limits

Solubility limit was defined as the concentration measured when the dissolution equilibrium of the chemical in the aqueous phase was reached. In theory, increasing temperature favours molecular agitation and thus incorporation and dissolution of the organic chemical in the aqueous solution. Hence, solubility is expected to increase with increasing temperature (Figure 24). On the contrary,

increasing salinity affects the organisation of water molecules around the chemical: in the presence of salts a proportion of water molecules is bound up in hydration spheres around the corresponding ions (e.g. Na^+, Cl^-) which generally lead to a decrease of water affinity for the chemical. This is commonly referred to the 'salting-out' effect (Millero 1996; Turner 2003). Hence, solubility is expected to decrease with increasing salinity (Figure 24). Note that seawater and artificial seawater solutions are equivalent in salting-out properties at the same molar concentration (Xie et al. 1997).

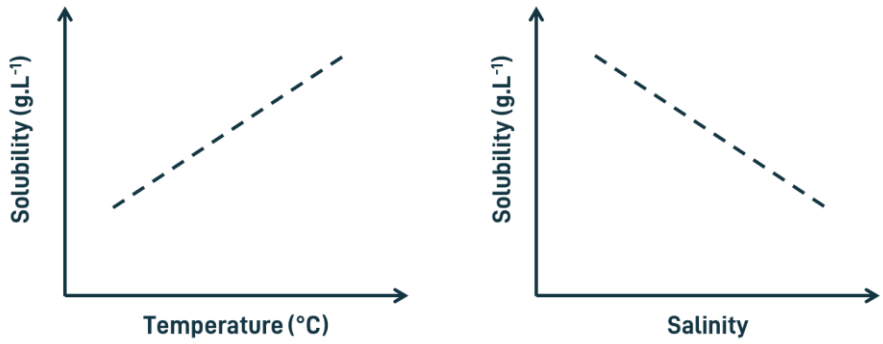

Figure 24. Theoretical effects of temperature and salinity on the hydrosolubility of HNS.

The experimental solubility limits assessed in this work are provided in Table 10. The corresponding data are also displayed against temperature and salinity (Figure 25 and Figure 26). Each value corresponds to the average concentration of all the sampling points of the plateau for each environmental conditions tested.

Solubility limits assessed in freshwater at 20°C were quite close to theoretical solubility with gaps in the range of 5 % for cyclohexane and vinyl acetate and 25 % for petroleum benzine. However this gap rises up to 38 % for acrylonitrile (Table 10, Figure 25). Additional tests could thus be repeated to confirm the value obtained for acrylonitrile in standard conditions.

Then, the effect of temperature on solubility limits was not as obvious as expected and no clear trend emerged (Figure 25 and Figure 26). Only dissolution of acrylonitrile appeared to be enhanced at higher temperature as solubility limits were 3, 8 and 12 % higher at 25°C than at 15°C in freshwater, 20 ‰ and 35 ‰ solutions, respectively (Table 10 and Figure 25). The other chemicals studied all displayed lower solubility limits at 25°C than at 15°C. Vinyl acetate concentrations decreased by 18, 20 and 17 % between 15°C and 25°C in freshwater, 20 ‰ and 35 ‰ solutions, respectively. Cyclohexane concentrations decreased by 56, 30 and 15 % between 15°C and 25°C in freshwater, 20 ‰ and 35 ‰ solutions, respectively. Finally for petroleum benzine, the decrease

measured was of 54, 48 and 45 % between 15 and 25°C in freshwater, 20 ‰ and 35 ‰ solutions, respectively. Surprisingly, the highest decreases were noticed in freshwater for both cyclohexane (56 %) and petroleum benzine (54 %).

Table 10. Solubility limits versus temperature and salinity. Data from the literature are from the HNS-database[3].

Acrylonitrile			
Temperature (°C)	**15**	**20**	**25**
	Solubility limits in water ($g.L^{-1}$)		
Freshwater	60.95 ± 3.73	48.86 ± 5.52	62.91 ± 4.45
S20	58.30 ± 3.10	54.01 ± 4.84	63.09 ± 3.28
S35	54.09 ± 5.25	50.50 ± 5.13	60.41 ± 1.88
Literature	-	79	-

Cyclohexane			
Temperature (°C)	**15**	**20**	**25**
	Solubility limits in water ($g.L^{-1}$)		
Freshwater	0.093 ± 0.008	0.052 ± 0.005	0.041 ± 0.004
S20	0.076 ± 0.011	0.043 ± 0.005	0.053 ± 0.008
S35	0.065 ± 0.005	0.037 ± 0.006	0.055 ± 0.009
Literature	0.045	0.055	-

Petroleum benzine			
Temperature (°C)	**15**	**20**	**25**
	Solubility limits in water ($g.L^{-1}$)		
Freshwater	0.035 ± 0.005	0.025 ± 0.004	0.016 ± 0.003
S20	0.027 ± 0.004	0.009 ± 0.001	0.014 ± 0.003
S35	0.022 ± 0.002	0.009 ± 0.001	0.012 ± 0.003
Literature	-	0.04	-

Vinyl acetate			
Temperature (°C)	**15**	**20**	**25**
	Solubility limits in water ($g.L^{-1}$)		
Freshwater	24.49 ± 4.71	21.09 ± 2.72	20.01 ± 3.40
S20	24.79 ± 1.16	22.40 ± 3.17	19.89 ± 2.37
S35	22.63 ± 2.89	15.54 ± 1.84	18.89 ± 2.06
Literature	-	20	-

The impact of salinity on solubility limits was generally in agreement with the 'salting-out' effect, as concentrations measured were decreasing with increasing salt concentrations (Table 10).

[3] https://manifests-project.eu/hns-database/

At 15°C, the solubility limit of acrylonitrile decreased by 4 % between freshwater and water at 20 ‰, by 7 % between water at 20 ‰ and 35 ‰ and by 11 % between freshwater and water at 35 ‰. Decreases in the same order of magnitude were observed for vinyl acetate that presented solubility limits lowered by 8 % between freshwater and water at 35 ‰. Note that variations observed are generally in the measurement error interval. This suggests that salinity only affects slightly the solubility limits of acrylonitrile and vinyl acetate at this temperature. Still at 15°C, cyclohexane and petroleum benzine showed solubility limits up to 30 and 37 % lower in water at 35 ‰ water than in freshwater, respectively.

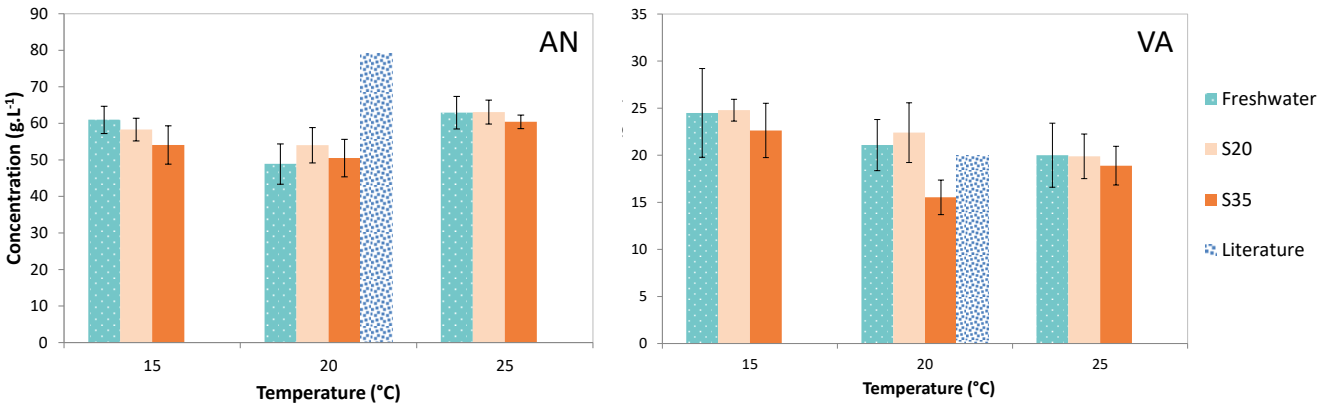

Figure 25. Solubility limits ($g.L^{-1}$) measured for acrylonitrile (AN) and vinyl acetate (VA). Values plotted correspond to the average concentration measured on the plateau for each environmental conditions tested. Note the different y-axis scales.

At 20°C, the solubility limits of acrylonitrile decreased by 6 % between water at 20 ‰ and 35 ‰. Increases in concentrations were observed between freshwater and water at 20 ‰ or 35 ‰ (11 and 3 %, respectively) but were in the measurement error range. However, vinyl acetate, cyclohexane and petroleum benzine showed sharper decreases in solubility limits with values up to 26, 29 and 64 % lower in water at 35 ‰ than in freshwater, respectively.

At 25°C, the solubility limit of acrylonitrile and vinyl acetate decreased by 4 and 6 % in water at 35 ‰ compared to freshwater, which is negligible when considering the measurement error range. However, the solubility limit of petroleum benzine sharply decreased by 25 % in water at 35 ‰ compared to freshwater. Finally, the solubility limit of cyclohexane was found to increase up to more than 30 % in water at 35 ‰ compared to freshwater without clear explanation (Table 10).

Two distinct behaviours could thus be observed: on one hand, acrylonitrile and vinyl acetate displayed negligible changes in solubility with increasing salinity (Figures 20, 21 and 25) whereas, on the other hand, cyclohexane and petroleum benzine seemed to be impacted more significantly

(Figures 22, 23 and 26). This makes sense in view of both the poor affinity of cyclohexane and petroleum benzine for water and the very low concentrations measured in the 3 aqueous solutions (Table 10): the smallest changes in the matrix should lead to a significant and visible impact on their dissolution process. On the contrary, acrylonitrile and vinyl acetate are the most hydrosolubles: changes in the matrix should not impact significantly their solubility considering their high concentrations in the 3 aqueous solutions.

Furthermore, Xie et al. (1997) have shown that the salting out effect is greater for organics solutes that display large molar volumes such as benzene, toluene or xylenes. Here the highest molar volumes were indeed found for cyclohexane (4.3 $L.mol^{-1}$) and petroleum benzine (5.5* $L.mol^{-1}$; *estimation as it is a mixture of xylenes) whereas acrylonitrile and vinyl acetate had the lowest (0.5 and 1.8 $L.mol^{-1}$, respectively). This is consistent with the two distinct behaviours that were observed at high salts concentrations.

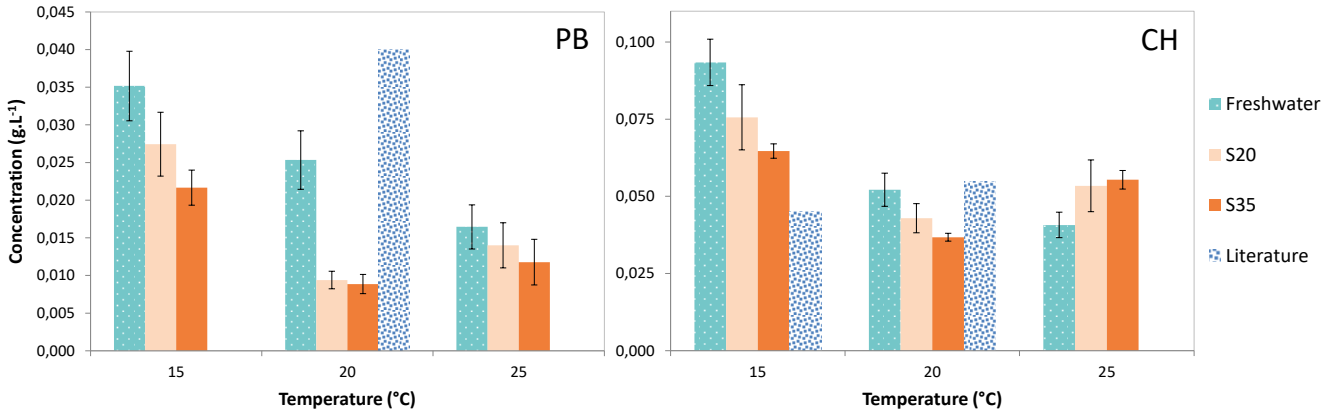

Figure 26. Solubility limits measured for petroleum benzine (PB) and cyclohexane (CH). Values plotted correspond to the average concentrations measured on the plateau. Note the different y-axis scales.

3.3.3. Relationship between solubility, temperature and salinity

Multiple regression analysis was used to model the conjugate effect of temperature and salinity on the solubility of each chemical in water (see Appendix 1; A1.1.3.4. Statistical analysis). Simple mathematical relationships were computed but are only valid in the experimental domain ($15 \leq T \leq 25°C$ and $0 \leq S \leq 35$ ‰) and for one specific chemical. Though it would be difficult to extrapolate such models to all chemicals, it should enable more realistic predictions of the weathering processes of the slick over an incident (e.g. dissolution model).

Acrylonitrile

The resulting model validated by a multiple regression analysis is provided in Table 11.

Table 11. Results of the multiple regression analysis describing the solubility of acrylonitrile with temperature and salinity.

Variable	Estimation	Standard error	T	Probability
Constant	187,567	11,5208	16,2807	0,0000
T: Temperature	-13,7553	1,17682	-11,6885	0,0000
S: Salinity	-0,105577	0,146661	-0,719869	0,4726
T^2	0,348078	0,0293122	11,8748	0,0000
TS	0,0168005	0,00591095	2,84226	0,0050
S^2	-0,00894722	0,00246447	-3,63048	0,0004

The R-squared statistic indicates that the fitted model explains 52.68% of the variability of C_{AN}. The largest probability value for the explanatory variables is 0.4726 and is associated with S. Since the probability value is greater than 0.05, this term is not statistically significant at the 95.0% confidence level. Thus, we may consider removing S from the model (Eq.2), in line with the behaviour observed and described in the previous paragraph.

$$C_{AN} = 187{,}567 - 13{,}7553\,T + 0{,}348078\,T^2 + 0{,}0168005\,TS - 0{,}00894722\,S^2 \quad \text{(Eq. 2)}$$

Cyclohexane

The resulting model for cyclohexane is provided in Table 12.

Table 12. Model describing solubility of cyclohexane with temperature and salinity.

Variable	Estimation	Standard error	T	Probability
Constant	0,467794	0,0312713	14,9592	0,0000
T: Temperature	-0,0369028	0,00326635	-11,2979	0,0000
S: Salinity	-0,00263296	0,000330257	-7,97244	0,0000
TS	0,00012149	0,0000135564	8,96182	0,0000
T^2	0,000797103	0,0000819765	9,72356	0,0000
S^2	-0,00000140003	0,0000058047	-0,241189	0,8100

The R-squared statistic shows that the fitted model explains 85.91 % of the variability in C_{CH}. The largest probability value for the explanatory variables is 0.8100 and is associated with S^2. Since the probability value is greater than or equal to 0.05, this term is not statistically significant at the 95.0% confidence level. Thus, the model can be simplified by removing S^2 (Eq. 3).

$$C_{CH} = 0{,}467794 - 0{,}0369028\,T - 0{,}00263296\,S + 0{,}00012149\,TS + 0{,}000797103\,T^2 \quad \text{(Eq. 3)}$$

Petroleum benzine

The resulting model for petroleum benzine is provided in Table 13.

Table 13. Model describing the solubility of petroleum benzine with temperature and salinity.

Variable	Estimation	Standard error	T	Probability
Constant	0,167121	0,00931803	17,9352	0,0000
T	-0,0126695	0,000933803	-13,5677	0,0000
S	-0,00117282	0,000127164	-9,22284	0,0000
TS	0,0000259746	0,0000052736	4,92541	0,0000
T^2	0,000270139	0,0000230624	11,7134	0,0000
S^2	0,00000865812	0,00000196695	4,40181	0,0000

The R-squared statistic shows that the fitted model explains 82.46 % of the variability in C_{PB}. Note that each probability value is lower than 0.05, i.e. statistically significant at the 95.0% confidence level. Hence the model is given by Eq.4:

$$C_{PB} = 0{,}167121 - 0{,}0126695\,T - 0{,}00117282\,S + 0{,}0000259746\,TS + 0{,}000270139\,T^2 + 0{,}00000865812\,S^2 \quad \text{(Eq. 4)}$$

Vinyl acetate

The resulting model for vinyl acetate is provided in Table 14.

Table 14. Model describing the solubility of vinyl acetate with temperature and salinity.

Variable	Estimation	Standard error	T	Probability
Constant	51,9373	12,3028	4,22158	0,0001
T	-2,69782	1,22179	-2,20809	0,0305
S	0,47665	0,203483	2,34246	0,0220
TS	-0,0103982	0,00716028	-1,45221	0,1509
T^2	0,057168	0,0296379	1,92888	0,0578
S^2	-0,0113751	0,00291975	-3,89592	0,0002

The R-squared statistic shows that the fitted model explains 45.94 % of the variability in C_{VA}. The probability values for TS^2 and T^2 are greater than 0.05 (0.1509 and 0.0578, respectively). Therefore, these terms are not statistically significant at the 95.0% confidence level and the model can be simplified as follows (Eq. 5):

$$C_{VA} = 51{,}9373 - 2{,}69782\,T + 0{,}47665\,S - 0{,}0113751\,S^2 \quad \text{(Eq. 5)}$$

3.4. Chemistry test bench

The evaporation and dissolution processes occurring when a chemical is released at sea surface were studied simultaneously using the chemistry test bench (Appendix 1; A1.1.4. Chemistry test

bench). The experimental data collected in the atmosphere and in the water column are provided in Appendices 2, 3 and 4. Concentrations in the water column are well above detections limits except for cyclohexane (CH: 0.25 mg.L^{-1}; PB: 0.05 mg.L^{-1}; VA: 0.05 mg.L^{-1}). The evaporation and dissolution processes are considered separately though they are occurring simultaneously. The global fate of the chemicals is then discussed.

3.4.1.Evaporation process

Cyclohexane and petroleum benzine have a density lower than seawater (0.78; Table 1), a theoretical solubility of 0.055 and 0.04 g.L^{-1} and a vapour pressure of ~10 and ~3 kPa, respectively. Of the 150 mL or 117 g of each product introduced into 80 L of seawater at 20°C, 4.4 and 3.2 g would be expected to dissolve based on theoretical values. Therefore, the disappearance of both cyclohexane and petroleum benzine would be expected to be mainly controlled by evaporation over dissolution in the water column. On the contrary, due to the greater solubility of vinyl acetate in water, a higher impact of dissolution in its fate would be expected as it was observed for lab tests.

Impact of wind velocity

The evaporation process was generally faster with stronger wind velocities. This is in agreement with the observations made using the wind tunnel (3.2.5). As an example, at 10°C and without wind, the slick of petroleum benzine disappeared around 3 h 40 after the spillage. At 6 m.s^{-1} and 8 m.s^{-1}, the slick remained 2 h and 1 h 30 on the surface, respectively (Figure 27). In fact, wind induces air renewal that favours the evaporation process. Note that vapour density are heavier than air for the 3 chemicals, suggesting that vapours tend to remain above the slick at low wind speed. Hence, care must be taken in case of incidents that would occur in low ventilated places (e.g. inside a ship).

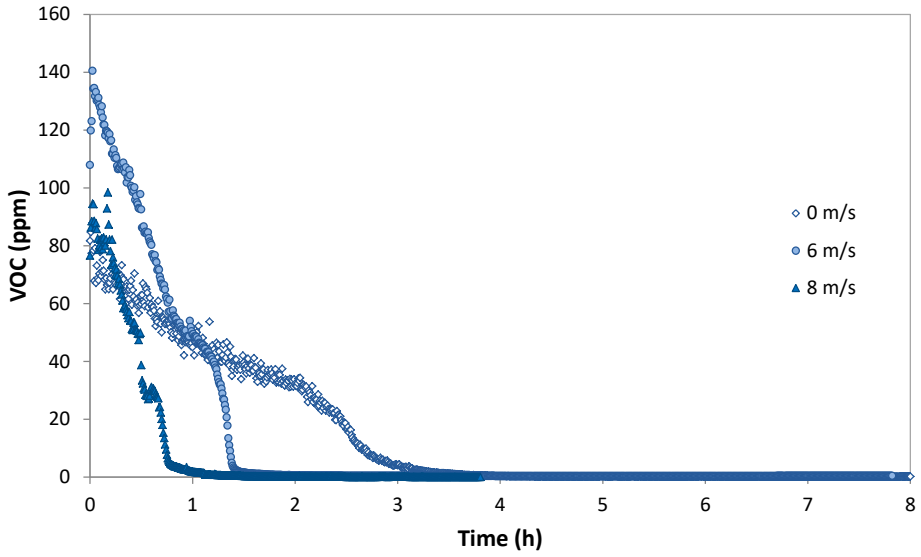

Figure 27. Concentrations of petroleum benzine measured in the atmosphere (water at 10°C).

Furthermore, the evaporation process was generally more intense at high wind velocities. For instance, the maximum concentrations measured for petroleum benzine at 10°C and 6 $m.s^{-1}$ (140 ppm) were 1.6 times higher than at 0.4 $m.s^{-1}$ (90 ppm). Nonetheless the highest concentration measured in the air was not reached at the highest wind velocity (8 $m.s^{-1}$) except for vinyl acetate. This might be linked to:

- a decrease of the chemical's temperature during the evaporation process as observed in the wind tunnel experiment (endothermic process). Such temperature decrease might have offset the evaporation kinetics which consequently lowered the concentration in the air at the beginning of the experiment;

- a higher sea surface agitation that might have induced a higher dissolution rate of the substance.

Impact of temperature

The impact of temperature on the evaporation process is described using the case of cyclohexane. Whether without wind or at 6 $m.s^{-1}$, the concentrations measured for cyclohexane in the air were higher at 20°C than at 10°C (Figure 28). For instance, without wind, the highest concentration measured at 10°C was of 1378 ppm while it reached 2719 ppm at 20°C. A similar feature was observed for vinyl acetate whatever the wind velocity. For petroleum benzine this was only the case without wind applied; at velocities of 6 and 8 $m.s^{-1}$ concentrations in the air where indeed much higher at 10°C than at 20°C (Figure 27 and Appendix 3). This might suggest that wind has as larger impact on the evaporation process in comparison with temperature.

When considering the persistence of the slick, the evaporation appeared to be systematically faster at higher temperature.

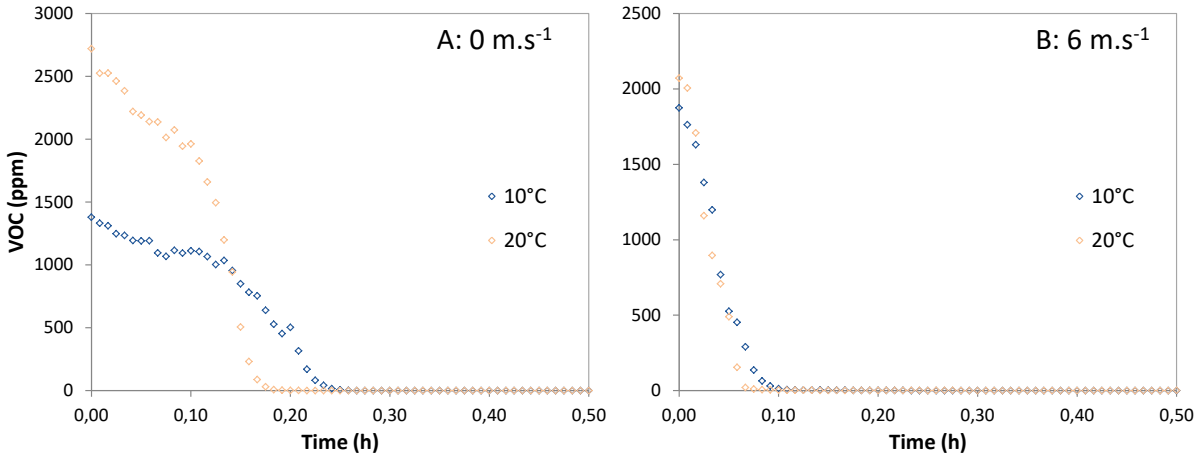

Figure 28. Concentrations of cyclohexane measured in the atmosphere at 10 and 20°C A) without wind and B) wind velocity of 6 $m.s^{-1}$. Note the two distinct y-axis scales.

3.4.2. Dissolution

Impact of wind velocity

Wind directly influences water surface agitation in the tank which infers greater contact between water and the chemical and, consequently, favours the dissolution process.

This was particularly the case for petroleum benzine at 10°C for which the dissolution was much higher at 8 m.s^{-1} than for the other wind conditions (Figure 29). The maximum concentration reached at this velocity was indeed 5 times greater (~ 1 mg.L^{-1}) than for the other conditions at the beginning of the experiment (~ 0.2 mg.L^{-1}; Appendix 3). Concentrations of petroleum benzine then decreased up to a concentration plateau of ~ 0.3 mg.L^{-1} (Appendix 3). A different behaviour was noticed at lower wind speed (0 and 6 m.s^{-1}) as dissolved concentrations were found to increase slightly up to the concentration plateau, i.e. from ~ 0.2 to ~ 0.3 mg.L^{-1} (Figure 29).

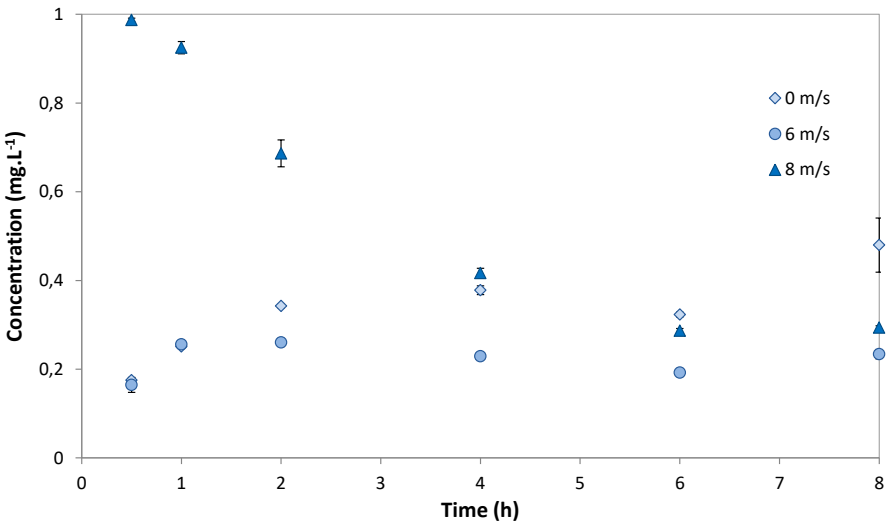

Figure 29. Concentration of petroleum benzine measured in the water column at 10°C.

Still at 10°C, the maximum concentration of vinyl acetate in water was reached without wind applied (8.5 mg.L^{-1}; Appendix 4) and remained almost constant over the course of the experiment (Figure 30). This is in agreement with the higher affinity of vinyl acetate with water. Different trends were then observed for stronger wind conditions. Indeed, at 6 m.s^{-1}, concentrations were found to slightly increase from ~ 3.7 to a maximum of ~ 4.4 mg.L^{-1} (Appendix 4). Though it seemed like a concentration plateau a slow decrease in concentrations could still be observed from 4.4 to 2.2 mg.L^{-1} over the duration of the experiment. At 8 m.s^{-1}, concentrations of vinyl acetate decreased more sharply and were up to 60 times lower 8 h after the spill (Figure 30). Such decreases could be explained by the evaporation of the HNS directly from the water column. Note that the trends observed at 6 and 8 m.s^{-1} are similar to those observed for petroleum benzine.

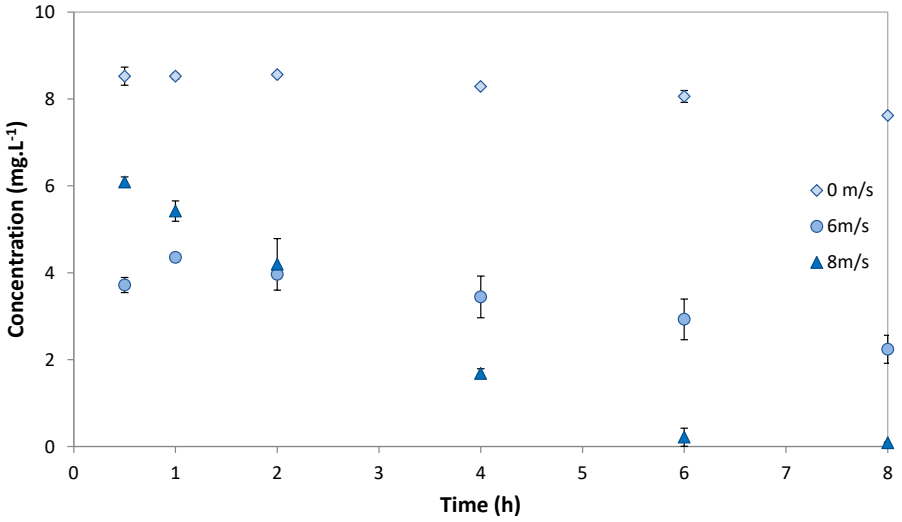

Figure 30. Concentration of vinyl acetate measured in the water column at 10°C.

Impact of temperature

Concentrations measured for cyclohexane and vinyl acetate in water were generally greater at 20°C than at 10°C whatever wind conditions. For instance at 6 and 8 $m.s^{-1}$, vinyl acetate displayed concentrations up to 60 % and 15 % greater at 20°C than at 10°C, respectively (Appendix 4; Figure 31). The dissolution process is thus favoured at higher temperatures for these two chemicals in line with theory (Figure 24).

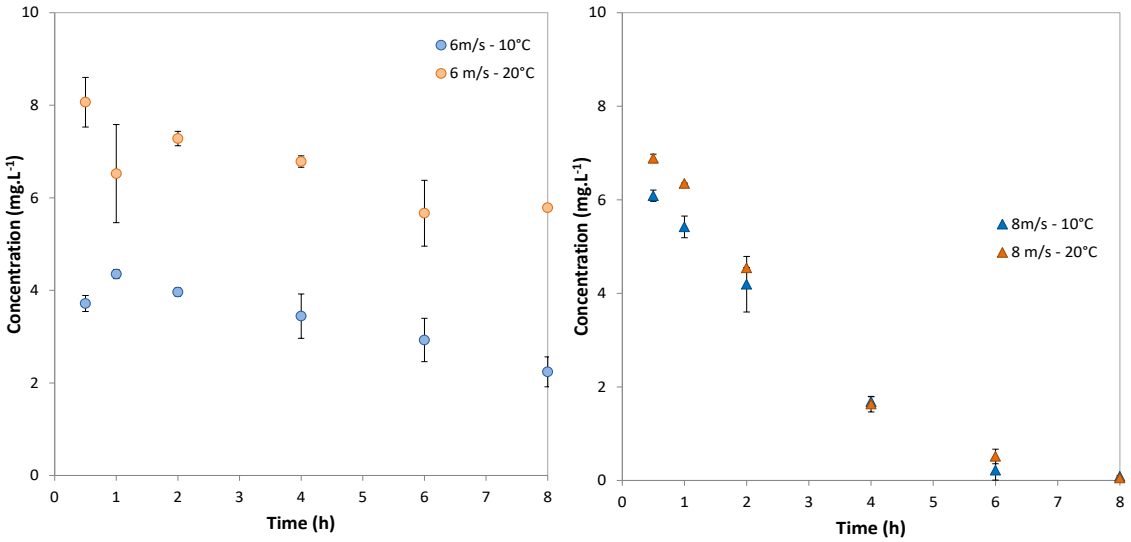

Figure 31. Concentrations of vinyl acetate at 10 and 20°C; Left: 6 $m.s^{-1}$; Right: 8 $m.s^{-1}$.

Surprisingly, concentrations of petroleum benzine in water were higher at 10°C than at 20°C. As petroleum benzine is FE, the evaporation process is favoured at 20°C; hence, petroleum benzine

evaporated faster at this temperature. As the slick is disappearing, the contact time between petroleum benzine and water is lowered and the dissolution is less important. At colder temperature, the dissolution is favoured due to a lower evaporation of the HNS. This phenomenon is also explained by the kinetics of the two processes: evaporation is a fast process whereas dissolution has a lower kinetics.

3.4.3. Overall fate

The global fate of each chemical was represented by normalised mass balance expressed versus time. The example of petroleum benzine and vinyl acetate is displayed in Figure 32 and Figure 33. Plots of VOC concentrations from PID measurements were first extrapolated to a straight line, from T0 to the time for which VOC concentrations measured were null. This enabled to estimate the time at which the slick was supposed to have fully disappeared. The amount of chemical evaporated was then deduced by subtracting the amount dissolved in water – calculated using the concentration of the dissolved fraction measured in seawater – to the total initial amount of chemical. Note that the persistence of the slick was not assessed experimentally, i.e. no internal standard was added to the chemical in the tank at the beginning of the experiment (e.g. tetracosane) and no sampling of the slick was performed at all. The data provided on slick persistence are thus a rough estimation to be considered with caution.

Whatever the chemical studied the dissolution process in the water column was much lower compared to the experimental solubility limits (3.3.2). This feature confirms that the evaporation kinetics is faster than the dissolution kinetics. During the first minutes or hours after the chemical is spilled, temperature seems to regulate the maximum amount of chemical evaporated (Figure 32), which is higher at 20°C, while the velocity of wind promotes directly the kinetic of evaporation.

In theory, the higher the wind speed, the faster the evaporation with lower concentration in the water column. However, coupling the PID and HS GC-MS data showed that dissolution could be more favoured at high wind velocities (e.g. petroleum benzine). The agitation of water surface generated by the wind explains this phenomenon. Furthermore, the chemistry bench is a pilot-scale tool: the representation of the natural space studied is not perfect. When a wind speed of 8 $m.s^{-1}$ is applied, water surface is in motion and can occasionally collide with the walls tank. This can create a stronger agitation that infers the formation of a vortex in the middle of the tank. This phenomenon prevents the chemical from naturally spreading and the slick surface is thus reduced. Consequently strong agitation in the chemistry test bench favours the dissolution and disadvantages the evaporation.

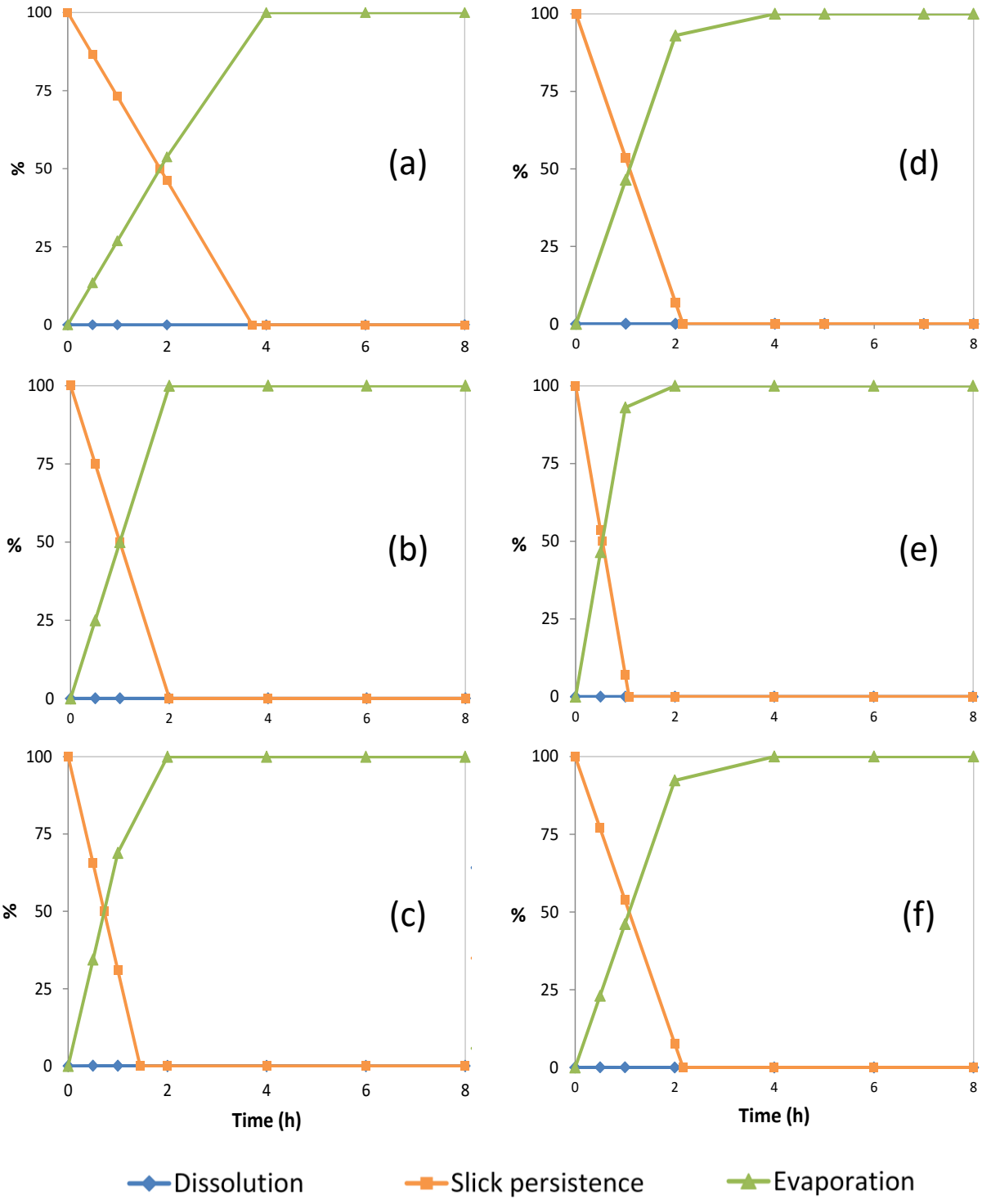

Figure 32. Normalised mass balance of petroleum benzine dissolved in water, remaining as a slick or evaporated at wind velocities of 0, 6 and 8 $m.s^{-1}$ at 10°C (a, b, c) and 20°c (d, e, f).

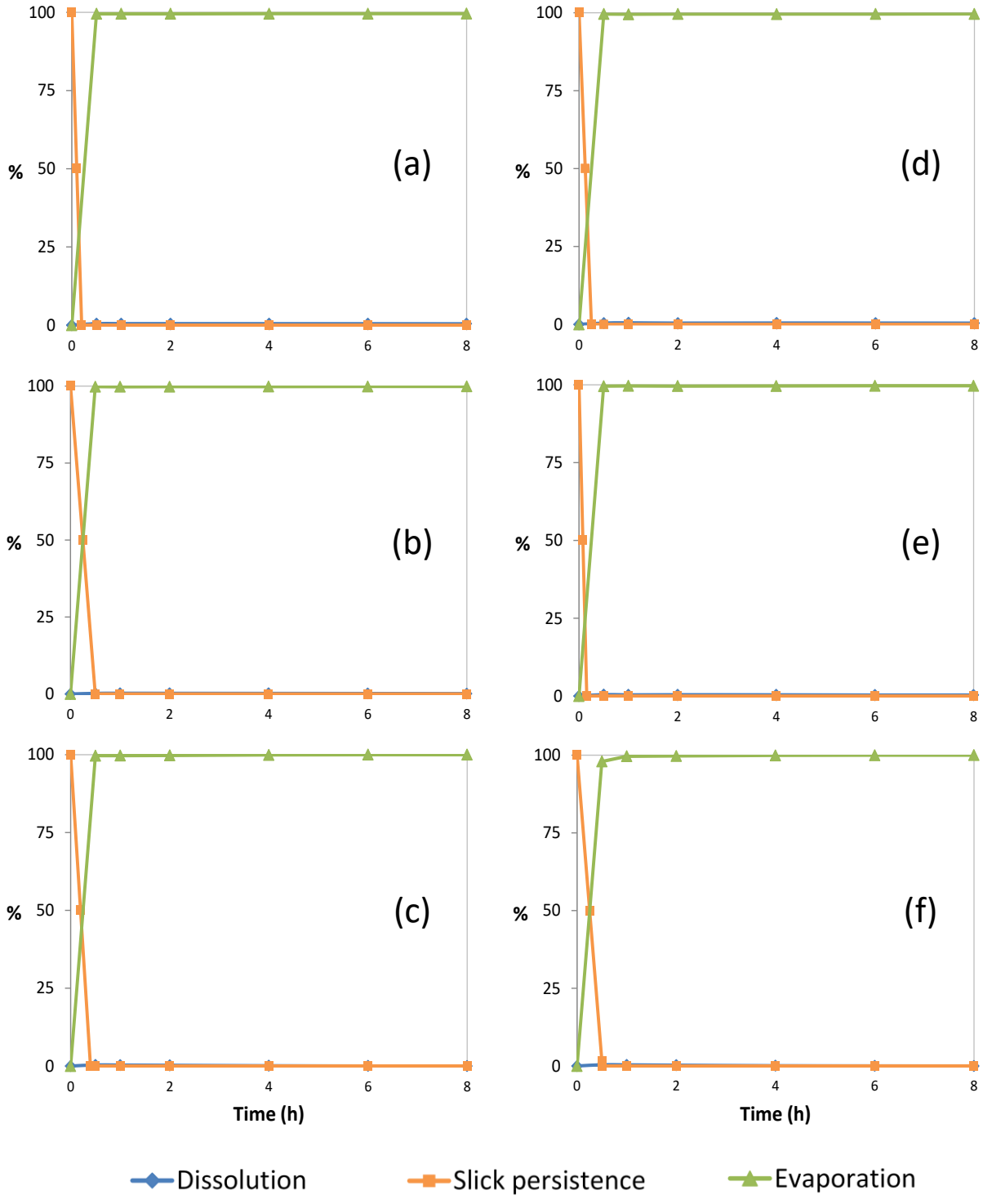

Figure 33. Normalised mass balance of vinyl acetate dissolved in water, remaining as a slick or evaporated at wind velocities of 0, 6 and 8 $m.s^{-1}$ at 10°C (a, b, c) and 20°c (d, e, f).

4. Conclusion

4.1. Scientific aspects

The mechanisms driving the evaporation and dissolution of a chemical from a slick on water surface were investigated through experimental tests at various scales.

Physical properties were first measured at 20°C in order to assess the reliability of the data available in literature. While specific gravity and surface tension were in agreement with literature, the experimental viscosities were greater than expected. This gap was due to the experimental device: the viscosities to be measured were too low for the concentric cylinder system used. The purchase of a specific measuring module is currently being considered. As expected, the measurements performed at various temperatures then showed that specific gravity, viscosity and surface tension were decreasing with increasing temperature.

The evaporation kinetics of the chemicals studied was then assessed at two scales: in the lab without wind applied and at pilot-scale using the wind tunnel. At lab scale, pure chemicals generally presented a constant evaporation rate over time. When released at the surface of seawater, the same chemicals displayed different behaviours and evaporation rates which were dependent on their vapour pressure and solubility in water. Apart from ETBE, longer evaporation rates were found, thus highlighting the competition between evaporation and dissolution processes. Regarding the binary mixtures studied, two behaviours were observed:

1. Each compound evaporated independently. In this case no particular hazard should be expected apart from the effects of a combined exposure to these two chemicals.
2. An apparent positive azeotropic mixture formed. In the field, this could lead to a greater risk of gas plume that could form faster than initially estimated by predictions models. Hence the notion of azeotrope should be popularized to responders for instance through the implementation of warning messages on available decision-support systems.

At pilot-scale, two different experiments were then carried out in order to assess the mass flow rate of chemicals. One performed at constant wind speed and the other one at increasing wind velocities. In both experiments it was observed that the evaporation process induces a sharp decrease of temperature that tends to reduce vapour pressure and, hence, evaporation. Depending on the chemical properties of the liquid, a stationary behaviour – where the liquid temperature remains constant – is then observed. At this stage, the evaporation rate becomes constant. This drop in liquid temperature should be taken into account in prediction models in order to improve prediction accuracy. The increase of wind velocity generally enhances evaporation kinetics as evidenced by higher mass flow rates.

The solubility of acrylonitrile, cyclohexane, petroleum benzine and vinyl acetate in water was characterised for different conditions of temperature and salinity of the aqueous phase. The data collected enabled to establish a mathematical relationship that models the conjugate effect of temperature and salinity on solubility. The most hydrosoluble chemicals presented the fastest dissolution kinetics and were not impacted significantly by increased salinity. On the contrary, the least hydrosolubles presented the slowest dissolution kinetics and higher solubility limits in freshwater than in salty water (20 and 35 ‰), in line with the 'salting' out effect and the SEBC. Solubility limits in seawater are usually unavailable in the literature; hence these experiments enabled to gain new data that will be included in the HNS database.

Eventually, the evaluation of the competition between evaporation and dissolution using the chemistry test bench enabled to confirm that the evaporation kinetics is faster than the dissolution kinetics. During the first minutes or hours after the chemical is spilled, temperature seems to regulate the maximum amount of chemical evaporated while the velocity of wind promotes directly the kinetic of evaporation.

Further work will be carried out using the wind tunnel with the objective to assess the evaporation kinetics of the same chemicals but spilt at the surface of seawater.

4.2. Operational aspects

The experimental tests carried out confirmed the theoretical behaviours described by the SEBC for five of the six chemicals studied, namely acrylonitrile (DE), ammonia aqueous (DE), cyclohexane (E), ETBE (E), petroleum benzine (FE). However, for vinyl acetate (ED), the observed experimental behaviour appears more driven by the evaporation process than suggested by the SEBC.

The wind tunnel experiment showed that increasing wind velocities involve higher evaporation rates of chemicals, i.e. a faster evaporation of the slick. The chemistry test bench enabled to confirm that the evaporation kinetics is faster than the dissolution kinetics.

In case of a release of a mixture of chemicals at sea the main priority is to check what are the substances involved and the risk of chemical reactions. Depending on the chemicals, azeotropic mixtures can form, involving either lower or greater boiling temperature than that of the pure constituents. Lower boiling temperatures entails greater and quicker risks of evaporation of the slick with associated toxic gas plumes. Wearing of appropriate PPE is thus highly recommended in such cases.

References

Alcaroa, L., Brandt, J., Giraud, W., Mannozzi, M., Nicolas-Kopec, A., 2021. Marine HNS response manual. *Multi-regional Bonn Agreement, HELCOM, REMPEC, Project Westmopoco* 1–321.

Andrade, E.N.D.C., 1930. The Viscosity of Liquids. *Nature* **125**, 309–310. https://doi.org/10.1038/125309b0

Armbruster, D.A., Tillman, M.D., Hubbs, L.M., 1994. Limit of detection (LOD)/limit of quantitation (LOQ): Comparison of the empirical and the statistical methods exemplified with GC-MS assays of abused drugs. *Clinical Chemistry* **40**, 1233–1238. https://doi.org/10.1093/clinchem/40.7.1233

Benbouzid, H., Le Floch, S., Stephan, L., Olier, R., Privat, M., 2012. Combined effects of salinity and temperature on the solubility of organic compounds. *The Journal of Chemical Thermodynamics* **48**, 54–64. https://doi.org/10.1016/j.jct.2011.11.020

Braconnier, R., Chaineaux, J., Triolet, J., Fontaine, J.R., Salle, B., 2008. Mesures du flux d'évaporation de liquides volatils dans des ambiances de travail - INRS. *Hygiène et sécurité du travail* 1–11.

Cattafesta, L., Bahr, C., Mathew, J., 2010. Fundamentals of wind-tunnel design. *Encyclopedia of Aerospace Engineering* 1–10.

Cunha, I., Moreira, S., Santos, M.M., 2015. Review on hazardous and noxious substances (HNS) involved in marine spill incidents - An online database. *Journal of hazardous materials* **285**, 509–516.

Davenport, A.G., 1965. The relationship of wind structure to wind loading. Proceedings of Conference 'Wind effects on buildings and structures' National Physical Laboratory 26-28 June 1963 HMSO 53–102.

Decelle, L., Nicolas, K., 2017. Conception d'une soufflerie de démonstration. *Projet de fin d'étude court. Polytech Lille* 1–19.

Du Noüy, P.L., 1919. A new apparatus for measuring surface tension. *The Journal of general physiology* **1**, 521.

Cedre, 2017. An innovative experimental device to assess the behavior of a chemical under controlled environmental parameters. *International Oil Spill Conference Proceedings* **2017**, 1287–1303. https://doi.org/10.7901/2169-3358-2017.1.1287

Gonczi, G., 2005. Comprendre la thermodynamique, Ellipses. ed.

Hamzah, H., Jasim, L.M., Alkhabbaz, A., Sahin, B., 2021. Role of honeycomb in improving subsonic wind tunnel flow quality: Numerical study based on orthogonal grid. *J. mechanical Engineering Research and Developments* **44**, 352–369.

Heymes, F., Aprin, L., Bony, A., Forestier, S., Cirocchi, S., Dusserre, G., 2013. An experimental investigation of evaporation rates for different volatile organic compounds. *Process Safety Progress* **32**, 193–198.

Jones, P.M., de Larrinaga, M.A.B., Wilson, C.B., 1971. The urban wind velocity profile. *Atmospheric Environment (1967)* **5**, 89–102. https://doi.org/10.1016/0004-6981(71)90164-8

Le Floch, S., Fuhrer, M., Merlin, F.-X., Péron, O., 2011. Experimental studies on the weathering of chemical products in open cells to predict their behaviour in case of a spill. Proceedings of International Oil Spill Conference (IOSC). Presented at the Proceedings of International Oil Spill Conference (IOSC).

Legrand, S., Poncet, F., Aprin, L., Parthenay, V., Donnay, E., Carvalho, G., Chataing-Pariaud, S., Dusserre, G., Gouriou, V., Le Floch, S., Le Guerroué, P., Hellouvry, Y.-H., Heymes, F., Ovidio, F., Orsi, S., Ozer, J., Parmentier, K., Poisvert, R., Poupon, E., Ramel, R., Schallier, R., Slangen, P., Thomas, A., Tsigourakos, V., Van Cappellen, M., Youdjou, N., 2017. Understanding HNS behaviour in the marine environment. *HNS-MS final report, part I* 1–152.

Mackay, D., Matsugu, R.S., 1973. Evaporation rates of liquid hydrocarbon spills on land and water. *The Canadian Journal of Chemical Engineering* **51**, 434–439.

Mamaca, E., Girin, M., Le Floch, S., el Zir, R., 2009. Review of chemical spills at sea and lessons learnt. A Technical Appendix to the INTERSPILL 2009 Conference White Paper "Are HNS spills more dangerous than oil Spills?"

Mamaca, E., Merlin, F., Le Floch, S., 2004. Experimental studies on the weathering of chemicals in a field trial to predict their behaviour in case of a spill.

Millero, F.J., 1996. Chemical oceanography, Second edition Boca Raton. ed. Florida.

Oke, T.R., 2002. Boundary layer climates, Second edition. ed. Routledge.

Palmer, S.J., 1976. The effect of temperature on surface tension. *Physics Education* **11**, 119. https://doi.org/10.1088/0031-9120/11/2/009

Poole, C., 2005. Gas chromatography, 2nd ed 'Elsevier.

Purnell, K., 2009. Are HNS more dangerous than oil spills? *White paper for the interspill conference and 4th IMO R&D Forum.*

Turner, A., 2003. Salting out of chemicals in estuaries: implications for contaminant partitioning and modelling. *Science of The Total Environment* **314–316**, 599–612. https://doi.org/10.1016/S0048-9697(03)00076-7

UNCTAD, 2022. Review of Maritime Transport 2022. *United Nations* 1–195.

UNCTAD, 2017. Review of Maritime Transport 2017. *United Nations* 1–137.

Ware, G.C., 1928. Surface tension of liquid ammonia and adsorption studies at its liquid vapor interface.

Xie, W.-H., Shiu, W.-Y., Mackay, D., 1997. A review of the effect of salts on the solubility of organic compounds in seawater. *Marine Environmental Research* **44**, 429–444.

Appendix 1

A.1. Material and methods

A.1.1. Chemicals

The list of chemicals studied is provided in Table A. As it is not possible to test every HNS a number were selected by the MANIFESTS Consortium based upon their SEBC behaviour, the frequency of transport and the potential hazards associated with transport and storage as well as the risks for human health. The selected chemicals could be seen as 'proxies' for other similar substances. Chemicals identified as 'evaporators' (E) in the Standard European Behaviour Classification (SEBC; Bonn Agreement 1994) in their short-term fate were given priority. All chemicals studied were of analytical grade.

Table A. List of HNS studied in the lab.

Chemicals	CAS number	SEBC	Boiling point (°C)	Vapour pressure (kPa)
Acrylonitrile	107-13-1	DE	77.4	11.5
Ammonia (32%)	1336-21-6	DE	38	47.4
Cyclohexane	110-82-7	E	80.7	10.3
Petroleum benzine (Naphta)	64742-82-1	FE	90	3 – 3.3
Tert-Butyl Ethyl Ether (ETBE)	637-92-3	E	73.1	20.6
Vinyl acetate	108-05-4	ED	72.7	12.0

A1.1.2. Evaporation

The evaporation kinetics of each chemical was first studied in the laboratory in standard conditions, i.e. at atmospheric pressure and 20°C and without any wind. The experiments enabled to assess and compare the evaporation kinetics of both the pure chemicals and the chemicals spilt at the sea surface. Various binary mixtures were also prepared in order to conduct preliminary evaporation tests, but without seawater. The impact of wind speed on the evaporation kinetics was then studied at pilot-scale using a brand-new experimental tool developed by Cedre in the framework of the project: the wind tunnel. Tests were performed on the same chemicals, except ammonia and ETBE. Results of both studies are presented in section 3.2.

A1.1.2.1. In lab experiment

All tests were carried out at Cedre in a temperature-controlled room set at 20°C, without any wind (extractor hood turned off). For pure chemicals, each experiment consisted in gently releasing

10 mL of one chemical in a pre-cleaned 9.8 cm diameter glass petri-dish. For tests with artificial seawater, the volume of chemical spilt at sea surface was the same. However, the volume of seawater was calculated based on the hydrosolubility of the HNS: the water was saturated to favour the evaporation process. Crystallizers of various sizes were used to hinder the accumulation of vapours above the slick (Table B). For binary mixtures, each experiment consisted in gently releasing 10 mL of each substance (V_{tot} = 20 mL) in the petri-dish. A 0.001 g-precision scale (Mettler – Toledo XS1203S) was used to monitor mass loss over time.

Table B. Main features of the glassware used for the experiments.

Glassware	Diameter (cm)	Volume of seawater (mL)
Petri dish	9.8	0
Crystallizer 1	6.7	30
Crystallizer 2	8.7	200
Crystallizer 3	11.2	500

A1.1.2.2. Wind tunnel

Assessing the impact of wind speed on the evaporation kinetics requires the establishment of a straight air flow whose mean speed and velocity profile are fully controlled. The wind tunnel was built by Cedre for this purpose. The air velocity profile corresponds with the variation of horizontal wind speed and direction with height, i.e. from the ground or the sea surface – where the wind speed is null – to the atmospheric boundary layer where the 'maximum' speed is reached (e.g. Jones et al. 1971). Such velocity profile depends on the roughness of the terrain over which the wind blows and directly impacts material transfer mechanisms at the surface of HNS slicks (Figure a).

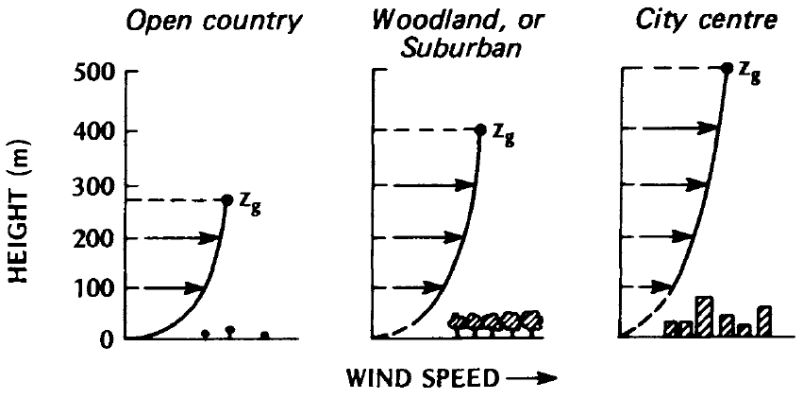

Figure a. Variation of the air velocity profile with surface roughness Z_0 (Davenport 1965; Oke 2002).

The experimental set up is displayed in Figure b. It consisted of a 3000$m^3.h^{-1}$ centrifugal hood fan with a cross-section of 25.4 cm x 29.2 cm placed at the entrance of a plywood tunnel of

approximately 4 m long. The fan speed was controlled using a frequency three-phase converter. A 30 cm-thick aluminium honeycomb (Euro-Composites) ensured that the air flow was homogenised with a fully developed turbulent flow. The honeycomb grid shape and porosity had to be selected carefully to ensure that the turbulence generated by the fan was reduced (Cattafesta et al. 2010; Decelle and Nicolas 2017): a hexagonal grid with cell size of 6.4 mm appeared as a good compromise (Hamzah et al. 2021). An opening was built in the floor to accommodate various dimensioned cuvettes inside the tunnel (up to 18 x 23 x 4 cm in which 500 mL of product could be evaporated).

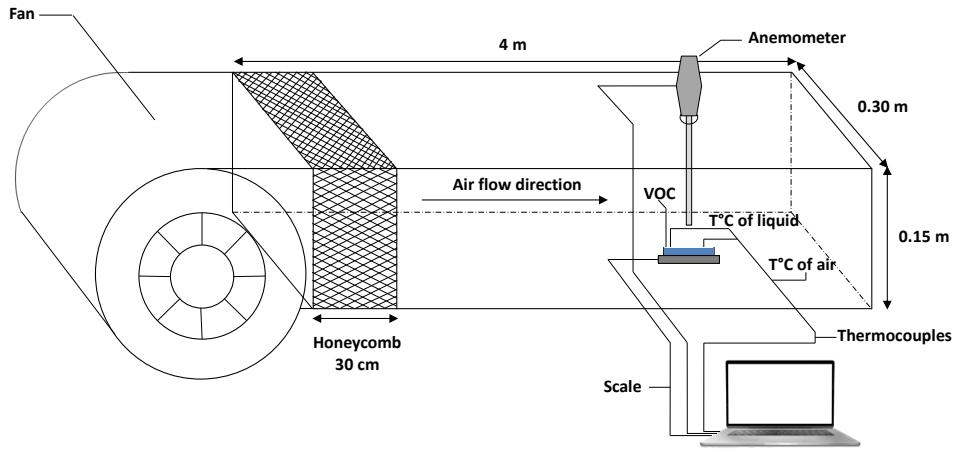

Figure b. Diagram of the wind tunnel adapted from Heymes et al. (2013).

All tests were carried out in order to compare the results initially collected in the laboratory. The same petri dish was filled with 10 mL of chemical pure and placed on top of the 0.001 g-precision scale (Mettler – Toledo XS1203S) inside the tunnel. The evaporation of the liquid was assessed by recording the mass loss of each chemical over time. The liquid and air temperatures were measured by three K-type thermocouples (Figure c). Mass and temperature data were recorded in real time at 2 Hz and 1 Hz, respectively. The air flow mean speed was measured using a hotwire anemometer (SEFRAM 9862) placed at 10 cm above the petri dish. Experimental air flow velocities were chosen in the range of 0.5 – 11 $m.s^{-1}$ (0.5; 1; 2; 3, 4; 7; 8 and 11 $m.s^{-1}$). No turbulence measurement was performed. However the dimensionless Reynolds number allowed characterising the flow pattern. It is dependent on the velocity of the wind (U_{air}), the hydraulic diameter of the vein (d) and the air kinematic viscosity (ν_{air}) and expressed as follows:

$$\mathrm{Re} = \frac{U_{air} \times d}{\nu_{air}}$$

In this case Re was ranging from 6,300 to 190,000 which is typical of a turbulent flow in a tunnel.

Figure c. Wide shot of the wind tunnel with a zoomed-in image of the petri dish and the operating sensors inside the gallery (temperature probes and anemometer): a) fan; b) tunnel; c) anemometer; d) thermocouples ; e) petri-dish and f) weighing scale.

A1.1.3. Dissolution

The dissolution process was investigated for acrylonitrile, cyclohexane, Petroleum benzine and vinyl acetate at various temperatures and salinities usually met in natural conditions. The experimental conditions selected were 15, 20 and 25°C for temperatures and 0, 20 ‰ and 35 ‰ for salinities. The objectives were to i) assess the dissolution kinetics and the solubility limit of each chemical in these experimental conditions and ii) establish a mathematical relationship modelling the hydrosolubility of each chemical as a function of temperature and salinity.

A1.1.3.1. Experimental protocol

Osmosis water was used as freshwater. Saline solutions were prepared from aquarium salts (Sea Salt, Aquaforest) and osmosis water. The day before the experiment, freshwater and saline solutions were transferred in glass bottles equipped with a draining tap (Figure d). Full glass bottles were then stored overnight at 15, 20 or 25°C in a temperature-controlled room. The day of the experiment each glass bottle was placed on a magnetic stirrer settled at low agitation (100 rpm) to avoid the formation of a vortex inside the solution.

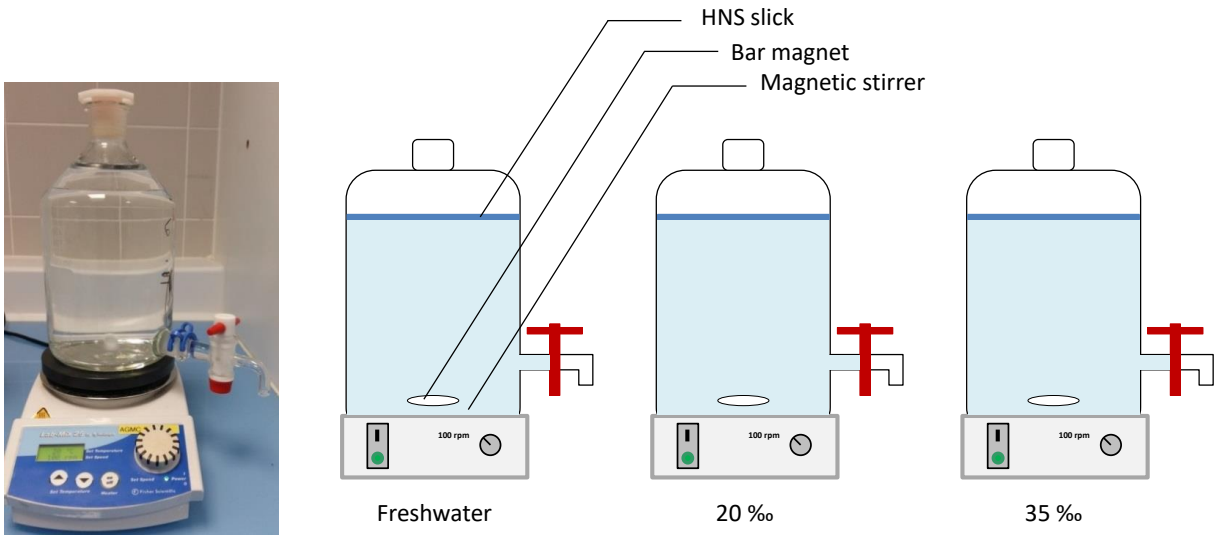

Figure d. Experimental set up to investigate the dissolution process of HNS. For each chemical and each temperature, 3 glass bottles were filled with freshwater and saline solutions at 20 ‰ and 35 ‰, respectively.

The amount of chemical spilt at the surface was calculated to be in large excess over the value of hydrosolubility found in literature. Samples were collected in triplicates in 20 mL baked brown glass flasks until the concentration of the triplicates was stable (for at least four sampling points). Sampling times were defined as a function of the theoretical hydrosolubility of chemicals and are summarised in Table C. T_0 corresponds to the sampling directly after the spill was made. Each flask was filled up to the top edge in order to flush out oxygen and to restrict the evaporation of the compound.

Table C. Sampling collection times.

Time (h) / HNS	0	0.25	0.5	1	2	4	8	24	32	48	56	72	80	96	104	144	156
Acrylonitrile	✓	✓	✓	✓	✓	✓	✓	✓	✓	✓	✓	✓	✗	✓	✗	✗	✗
Cyclohexane	✓	✗	✗	✓	✗	✓	✓	✓	✓	✓	✓	✓	✓	✓	✓	✓	✓
Petroleum benzine	✓	✗	✗	✓	✗	✓	✓	✓	✓	✓	✓	✓	✓	✓	✓	✓	✓
Vinyl acetate	✓	✗	✓	✓	✓	✓	✓	✓	✓	✓	✓	✗	✗	✗	✗	✗	✗

A1.1.3.2. Analytical method

Considering the low boiling point (< 100°C) and the high vapour pressure (> 10 kPa) of the 4 chemicals studied, all samples were analysed by gas chromatography (GC) coupled with Mass

Spectrometry (MS) and headspace (HS) extraction. The gas chromatrograph (Agilent 7890A, USA) was equipped with a Combipal MPS2 multifunction injector (Gerstel, Switzerland) in splitless mode. The analysis was performed after dilution of samples in freshwater or in artificial seawater (dilution factor: 500, 2, 10 and 200 for acrylonitrile, cyclohexane, petroleum benzine and vinyl acetate, respectively). Briefly, 10 mL of liquid sample were placed in a sealed vial and heated at 60°C until the equilibrium was reached between the liquid and vapour phases. A volume of 1 mL of the vapour-phase mixture was then withdrawn through a 1 mL-gas-tight syringe and transferred to the chromatograph for separation and analysis of the components (Poole 2005). A HP – 5MS (5%-phenyl)- methylpolysiloxane capillary column (Agilent technologies) of 30 m length, 0.25 mm in inner diameter and 1 µm in film thickness was used. Experimental conditions are summarised in Table D.

An internal standard calibration method was used to normalize systematic errors such as variable sample injection volumes or bias induced by sample preparation (Poole 2005). The concentration of the substance to be investigated (analyte) was determined by comparing the ratio of the peak areas of the analyte and the internal standard in the samples with the ratio of the peak areas of the analyte and the internal standard in the stock solutions (Poole 2005). Blanks were prepared using a matrix identical to that of samples but without the analyte. The limit of detection (LOD) and the limit of quantification (LOQ) were defined as the mean blank value plus 3 and 10 SDs, respectively (Armbruster et al. 1994).

Table D. GC experimental conditions.

HNS	Acrylonitrile	Cyclohexane	Petroleum benzine	Vinyl acetate
Oven program	40 °C for 1 min 10°C.min^{-1} to 100°C for 2 min 80°C.min^{-1} to 230°C for 0 min	40°C for 1 min 10°C.min^{-1} to 85°C for 1 min 10°C.min^{-1} to 100°C for 2 min 100°C.min^{-1} to 250°C for 0 min	40°C for 1 min 25°C.min^{-1} to 250°C for 0 min	40°C for 1 min 10°C.min^{-1} to 100°C for 0 min then 50°C.min^{-1} to 250°C for 0 min
Carrier gas	He	He	He	He
Flow	1 mL.min^{-1}	1 mL.min^{-1}	1 mL.min^{-1}	1 mL.min^{-1}
Inlet temperature	225°C	225°C	225°C	225°C
Injection volume	1 mL	1 mL	1 mL	1 mL
Selected ion monitoring (SIM)	53 m/z	84 m/z	91 m/z	43 m/z
Internal standard	Propionitrile	Heptane	Toluene D8	Ethyl acetate
Concentration of the internal standard	10 mg.L^{-1}	2 mg.L^{-1}	0.2 mg.L^{-1}	10 mg.L^{-1}

A1.1.3.3. Expected results

In theory and as shown in Figure e, the concentration of each chemical studied should increase gradually over time until a constant is reached (hereafter the 'plateau'). The average value of all the measurement points of the plateau along with the standard deviation was considered as the solubility limit. The dissolution kinetics corresponded to the time needed to reach the concentration plateau for each compound studied.

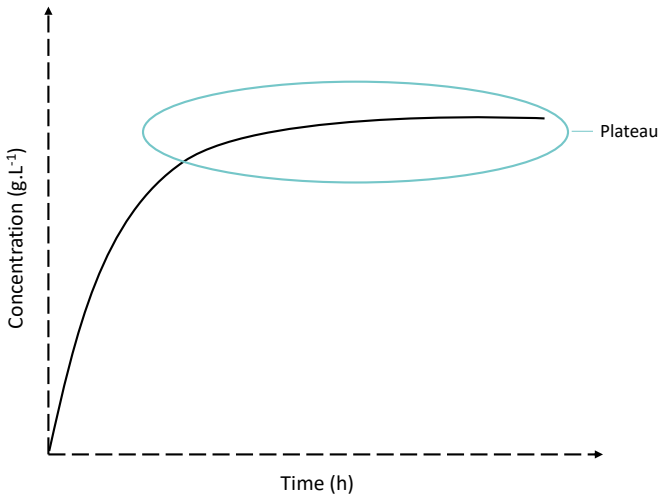

Figure e. Expected evolution of the concentration of chemicals with time.

A1.1.3.4. Statistical analysis

Once concentrations of chemicals were assessed, a multiple regression analysis was performed on the data of the plateau using the Statgraphics software. This enabled to compute a mathematical relationship that models the solubility of each chemical in aqueous phases with temperature and salinity.

A1.1.4. Chemistry test bench

This experimental device was used to study the transfer kinetics of chemicals from the water surface into the atmosphere and the aquatic environment in controlled conditions (Cedre 2017). The system enables characterising the evaporation and dissolution processes occurring simultaneously and to identifying which one is predominant. It is designed to recreate the effects of several environmental parameters (water temperature, wind speed, sunshine and surface agitation). The device is equipped with a 50 cm diameter 316 L cylindrical stainless steel tank. Part of the tank is made of tempered glass that enables the observation of HNS slicks during experimentations

(Figure f). All tests were performed in filtered and UVIR seawater. Three chemicals were studied: cyclohexane, petroleum benzine and vinyl acetate.

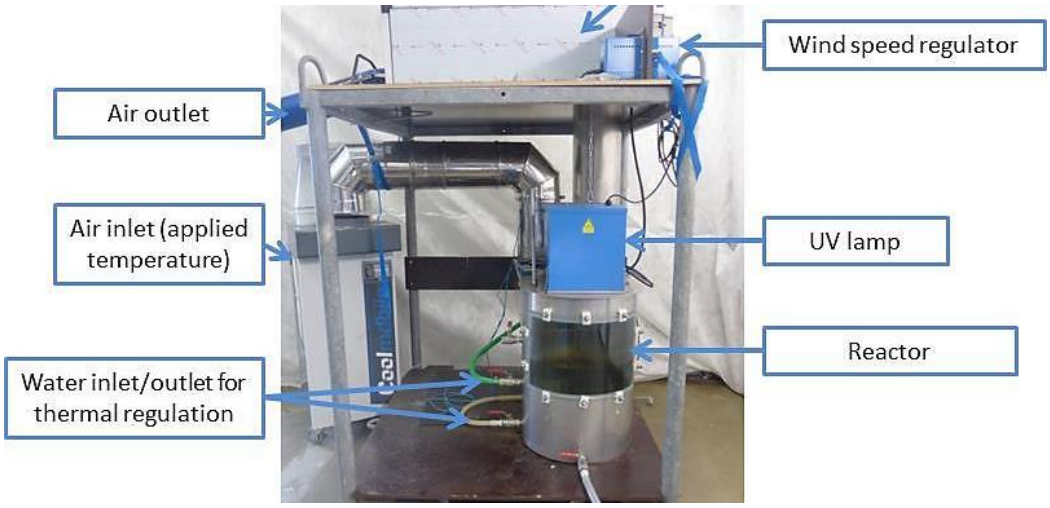

Figure f. Chemistry test bench (Legrand et al. 2017).

The volume of seawater introduced in the reactor was of 80 L. The temperature of seawater was set using a SIEBEC M15 external pump connected to a TECO TR20 cooling unit and monitored using a K-type thermocouple immerged in water. The set point temperature was adjusted in order to obtain a temperature of 10 ± 1 °C or 20 °C ± 1 °C in the water column. A constant velocity of wind was applied using a ventilation unit and an Atlantic IP 65 regulator. A multisensory anemometer MiniAir20 (Schiltknecht) was placed at 5 cm above the water surface to check wind speed before starting the experiment. Air temperature was regulated using a mobile reversible air-conditioning unit CoolMobile E25. Due to the high volatility of the chemicals tested, the UV lamp usually used to simulate solar radiations was not used. Indeed, the power of the lamp is not adapted to this type of product, and the resulting heat tends to strongly accelerate the evaporation process of the HNS slick.

Six environmental conditions were tested:

- Three wind velocities (0.4 $m.s^{-1}$, 6 $m.s^{-1}$ and 8 $m.s^{-1}$);
- Two temperatures (10°C and 20°C).

Note that it was not possible to reach zero for the wind speed because of the constant evacuation of the vapours emanating from the slick outside the tank. For information purpose a wind velocity of 6 $m.s^{-1}$ corresponds to 4 on the Beaufort scale and enables reproducing a moderate breeze. A wind velocity of 8 $m.s^{-1}$ corresponds to 5 on the Beaufort scale and enables reproducing a cool breeze.

As soon as the temperature was stable in the tank, 150 mL of HNS were gently poured at the surface of seawater. Concentrations of VOC in the atmosphere were continuously monitored above water using a Photo Ionization Detector (PID) MiniRAE 3000 equipped with a lamp of 10.6 eV. The calibration of the PID was performed with isobutylene and a factor of correction was applied, depending on the HNS studied. The air admission tip was placed 10 cm above water surface and VOC concentrations recorded every 10 seconds. The evaporation of the HNS slick was considered as ended as soon as the signal of the PID had reached zero.

Water sampling was performed at different times to monitor the solubilisation of the chemical over time (Table E). As cyclohexane is more volatile, samples were collected at higher frequency in the first hour following the spill. Ventilation was systematically turned off before each sampling. As soon as the water surface was stable, 150 mL were collected at around 20 cm below the surface for further analyses by HS-GC-MS as described in A1.1.3.2.

Table E. Sampling times for each of the 6 conditions tested.

Chemical	T_1 (h)	T_2 (h)	T_3 (h)	T_4 (h)	T_5 (h)	T_6 (h)
Cyclohexane	0.25	0.5	0.75	1	2	-
Petroleum benzine	0.5	1	2	4	6	8
Vinyl acetate	0.5	1	2	4	6	8

Appendix 2

Experimental data for cyclohexane

Concentrations measured for cyclohexane in the water column are provided in the following table.

Concentrations measured in the atmosphere are provided at 10 and 20°C (graphs).

Temperature	Cyclohexane 10°C						Cyclohexane 20°C					
Wind (m.s^{-1})	0		6		8		0		6		8	
Time (h)	C (mg.L^{-1})	SD	C (mg.L^{-1})	SD	C (mg.L^{-1})	SD	C (mg.L^{-1})	SD	C (mg.L^{-1})	SD	C (mg.L^{-1})	SD
0,25	0,1109	0,0308	< LOD	0,0016	0,0500	0,0730	0,1470	0,0757	< LOD	0,0064	0,0669	0,0060
0,5	0,0103	0,0524	< LOD	0,0005	0,0190	0,0105	0,1217	0,0802	< LOD	0,0065	0,0735	0,0168
0,75	0,0309	0,0708	< LOD	0,0020	0,0212	0,0036	0,1448	0,1019	0,0019	0,0104	0,1138	0,0030
1	0,0253	0,0434	< LOD	0,0002	0,0140	0,0068	0,2012	0,1245	< LOD	0,0044	0,1015	0,0010
2	0,0237	0,0824	< LOD	0,0008	< LOD	0,0010	0,1300	0,2013	< LOD	0,0047	0,0728	0,0077

10°C

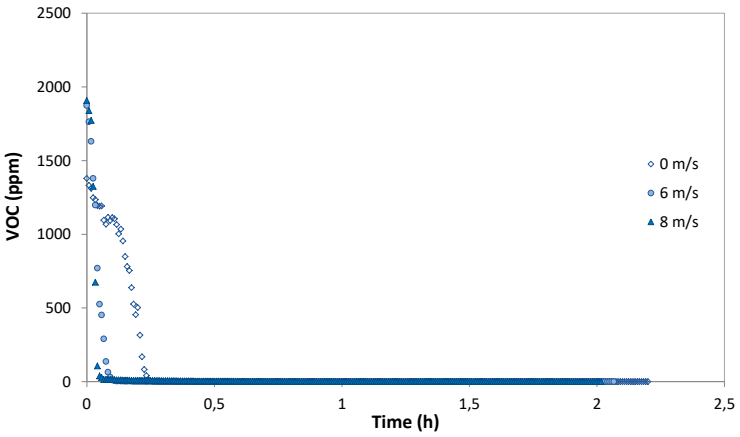

20°C

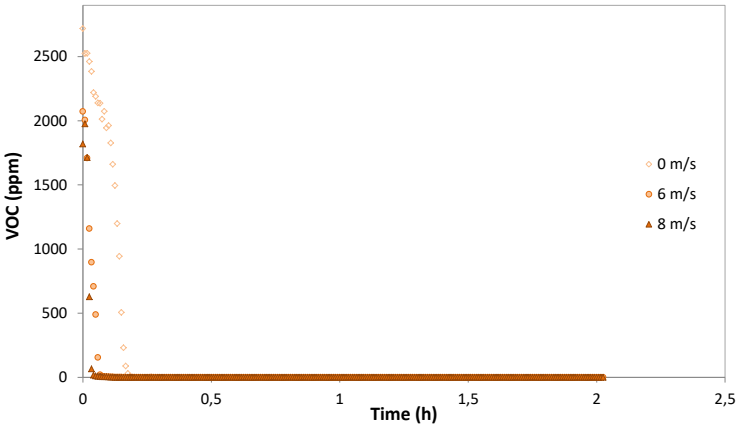

Appendix 3

Experimental data for petroleum benzine

Concentrations measured for Petroleum benzine in the water column are provided in the following table.

Temperature	Petroleum benzine 10°C						Petroleum benzine 20°C					
Wind (m.s^{-1})	0		6		8		0		6		8	
Time (h)	C (mg.L^{-1})	SD	C (mg.L^{-1})	SD	C (mg.L^{-1})	SD	C (mg.L^{-1})	SD	C (mg.L^{-1})	SD	C (mg.L^{-1})	SD
0,5	0,175	0,006	0,165	0,017	0,987	0,004	0,140	0,026	0,076	0,009	0,335	0,126
1	0,251	0,002	0,256	0,005	0,925	0,014	0,172	0,003	0,066	0,000	0,149	0,032
2	0,342	0,005	0,260	0,004	0,686	0,030	0,148	0,004	0,084	0,033	0,107	0,029
4	0,378	0,010	0,229	0,006	0,417	0,011	0,135	0,001	0,074	0,022	0,087	0,008
6	0,323	0,006	0,193	0,005	0,287	0,005	0,128	0,016	0,071	0,015	0,086	0,023
8	0,480	0,061	0,234	0,011	0,294	0,004	0,103	0,007	0,066	0,002	0,072	0,005

10°C

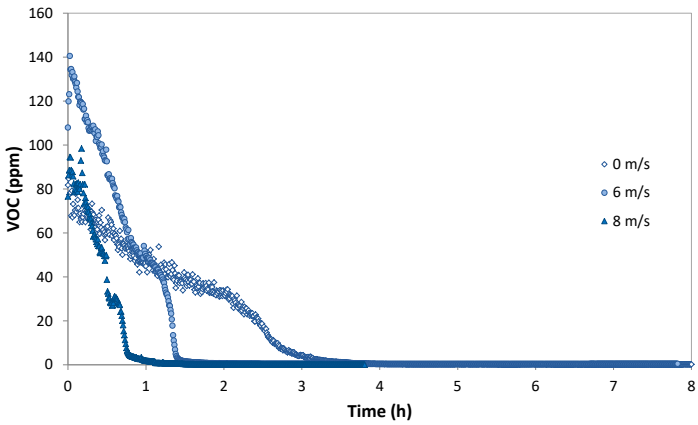

20°C

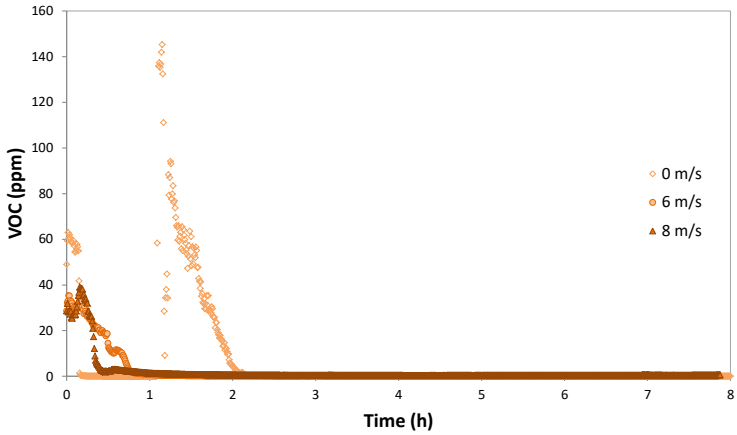

The curious shape of the curve was caused by an obstruction of the PID's sampling pipe inside the reactor: an intervention on the device was required during the running experiment.

Appendix 4

Experimental data for vinyl acetate

Concentrations measured for vinyl acetate in the water column are provided in the following table. Concentrations measured in the atmosphere are provided at 10 and 20°C (graphs).

Temperature	10°C						20°C					
Wind (m.s^{-1})	0		6		8		0		6		8	
Time (h)	C (mg.L^{-1})	SD	C (mg.L^{-1})	SD	C (mg.L^{-1})	SD	C (mg.L^{-1})	SD	C (mg.L^{-1})	SD	C (mg.L^{-1})	SD
0,5	8,52	0,21	3,72	0,17	6,09	0,12	7,37	1,43	8,06	0,54	6,88	0,09
1	8,52	0,07	4,35	0,10	5,42	0,23	8,87	0,12	6,52	1,06	6,35	0,01
2	8,56	0,01	3,96	0,09	4,19	0,59	7,23	1,62	7,28	0,16	4,54	0,01
4	8,28	0,01	3,44	0,48	1,68	0,11	7,79	0,26	6,78	0,12	1,63	0,17
6	8,06	0,14	2,93	0,47	0,22	0,21	7,48	0,08	5,67	0,71	0,51	0,16
8	7,62	0,04	2,24	0,32	0,09	0,02	7,10	0,09	5,79	0,07	0,05	0,00

10°C

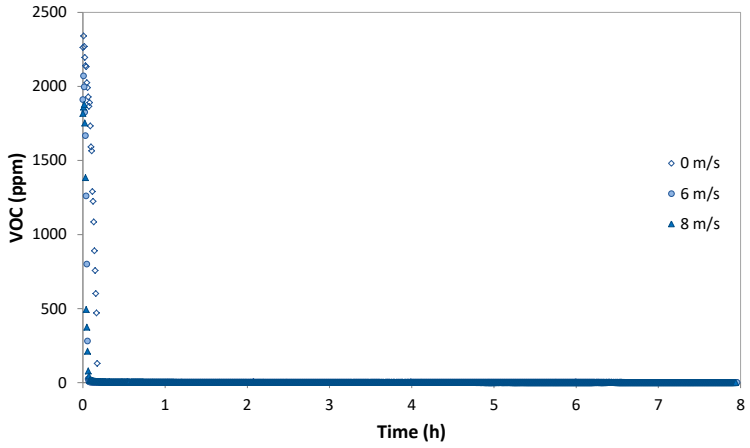

20°C

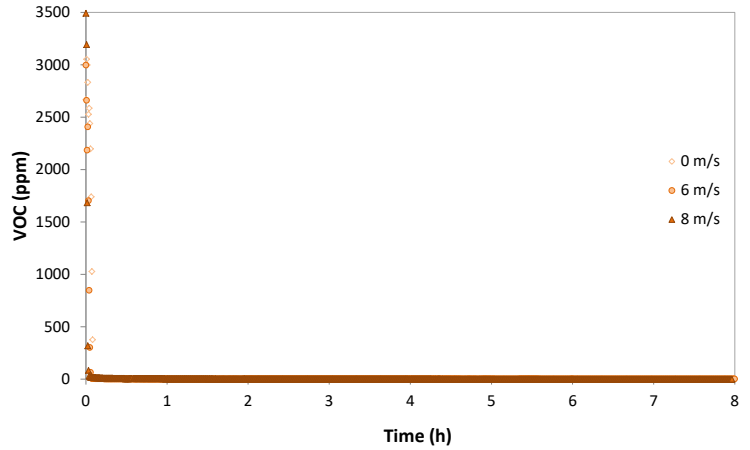

PAGE INTENTIONALLY LEFT BLANK

Co-funded by the European Union